Manuscript DB16-1252 - revised

MCL-1 is a key anti-apoptotic protein in human and rodent pancreatic β-cells

Kira Meyerovich[1#], Natalia M. Violato[1#], Makiko Fukaya[1], Violette Dirix[2], Nathalie Pachera[1], Lorella Marselli[3], Piero Marchetti[3], Andreas Strasser[4,5], Decio L. Eizirik[1], Alessandra K. Cardozo[1*]

[1] ULB Center for Diabetes Research, Medical Faculty, Université Libre de Bruxelles (ULB), Brussels, Belgium;[2]Laboratory of Vaccinology and Mucosal Immunity, ULB Brussels, Belgium[3]Department of Clinical and Experimental Medicine, Islet Laboratory, University of Pisa, Pisa, Italy; [4]The Walter and Eliza Hall Institute of Medical Research, Parkville, Australia; [5]The Department of Medical Biology, University of Melbourne, Parkville, Australia

# K.M. and N.M.V. contributed equally to this work

*Address correspondence to: Alessandra K. Cardozo, ULB Center for Diabetes Research, Université Libre de Bruxelles - Route de Lennik, 808 - CP 618 – 1070 - Brussels – Belgium - akupperc@ulb.ac.be - phone + 32 2 555 6204; fax + 32 2 555 6239

Running title: MCL-1: the key anti-apoptotic protein in β-cells

Conflict of interest: The authors declare no conflict of interest.

Word count: abstract: 199 words; main text: 4067 words; main figures: 7 (+ 4 supplemental); supplemental tables: 3

Diabetes Publish Ahead of Print, published online June 30, 2017

ABSTRACT

Induction of endoplasmic reticulum stress and activation of the intrinsic apoptotic pathway is widely believed to contribute to β-cell death in type 1 diabetes (T1D). MCL-1 is an anti-apoptotic member of the BCL-2 protein family, whose depletion causes apoptosis in rodent β-cells *in vitro*. Importantly, decreased MCL-1 expression was observed in islets from T1D patients. We report here that MCL-1 downregulation is associated with cytokine-mediated killing of human β-cells, a process partially prevented by MCL-1 overexpression. By generating a β-cell specific *Mcl-1* knockout mouse strain (*βMcl-1*KO**)**, we observed that, surprisingly, MCL-1 ablation does not affect islet development and function. β-cells from *βMcl-1*KO mice were, however, more susceptible to cytokine-induced apoptosis. Moreover, *βMcl-1*KO mice displayed higher hyperglycaemia and lower pancreatic insulin content after multiple low dose streptozotocin treatment. We found that the kinase GSK3β, the E3 ligases MULE and βTrCP and the deubiquitinase USP9x, regulate cytokine-mediated MCL-1 protein turnover in rodent β-cells. Our results identify MCL-1 as a critical pro-survival protein for preventing β-cell death and clarify the mechanisms behind its downregulation by pro-inflammatory cytokines. Development of strategies to prevent MCL-1 loss in the early stages of T1D may enhance β-cell survival and thereby delay or prevent disease progression.

Secretion of pro-inflammatory cytokines by immune cells contributes to β-cell death in type 1 diabetes (T1D) (1) and exposure of human islets *in vitro* to the pro-inflammatory cytokines interleukin-1β (IL-1β) and interferon-γ (IFN-γ) induce global changes in gene expression (2) that are remarkably similar to those observed in laser-captures islet cells from T1D patients (3). One of the mechanisms involved in cytokine-mediated β-cell killing is the induction of endoplasmic reticulum (ER) stress and the consequent activation of the intrinsic (mitochondrial) apoptotic pathway (4; 5). The intrinsic apoptotic pathway is regulated by the B-cell lymphoma 2 (BCL-2) family of proteins, which is divided into three groups: the anti-apoptotic members (e.g. MCL-1, BCL-2), the pro-apoptotic BH3-only proteins (e.g. BIM, DP5/HRK, PUMA) and the multi-BH (BCL-2 Homology) domain pro-apoptotic protein BAX and BAK (5; 6).

MCL-1 prevents apoptosis induced by BIM and PUMA, two BH3 only proteins that contribute to ER stress and inflammatory cytokine induced β-cell killing (5; 7-9). MCL-1 protein is expressed in rodent β-cells and cytotoxic insults that induce β-cell apoptosis, such as inflammatory cytokines, reduce MCL-1 protein expression in these cells (7; 10; 11). Importantly, MCL-1 overexpression protects primary rat β-cells against diverse cytotoxic conditions (7; 11). Moreover, overexpression of microRNA-29 (miR-29) promotes β-cell death by decreasing MCL-1 protein expression (10). Interestingly, abnormally reduced expression of MCL-1 is present in islets from T1D patients infected with a diabetogenic enterovirus, suggesting that defects in MCL-1 expression play a role in the development of human diabetes (12).

We have previously shown that MCL-1 protein expression is reduced in inflammatory cytokine-treated β-cells due to the combined actions of ER stress-mediated translation arrest and JNK-induced MCL-1 phosphorylation, which was reported to prime this protein for ubiquitination and proteasomal degradation (11). Given the importance of MCL-1 in the survival of β-cells, the aim

of the present study was to clarify its role in human β-cells, as well as in an *in vivo* murine model of diabetes and to determine the mechanisms involved in the post-translational regulation of MCL-1 protein levels in β-cells. We found that inflammatory cytokine-mediated MCL-1 downregulation contributes to the death of human β-cells and that this can be partially inhibited by ectopic MCL-1 overexpression. We generated a β-cell specific *Mcl-1* knockout mouse line (*βMcl-1*KO**)** and observed that these mice were more hyperglycaemic and had lower insulin content after multiple low dose streptozotocin (MLDSTZ) treatment. Mechanistic studies in rat β-cells indicated that the kinase GSK3β, the E3 ligases MULE and βTrCP, as well as the deubiquitinase, USP9X, regulate inflammatory cytokine-mediated MCL-1 reduction in β-cells. Overall, our results identify MCL-1 as an important guardian against β-cell death and clarify the mechanisms behind its regulation by pro-inflammatory cytokines.

RESEARCH DESIGN AND METHODS

Materials

The cytokine concentrations utilised were based on prior studies (13-15) and are described in Suppl. Table 1. The GSK3α/β inhibitors SB216763 and BIO (Sigma-Aldrich, Diegem, Belgium) were dissolved in DMSO (1:1000) and used at 5 μmol/L or 1 μmol/L, respectively. For immunoprecipitation experiments, cells were treated with the proteasome inhibitor MG-132 (Sigma-Aldrich, Diegem, Belgium) at 1 μmol/L.

Generation and characterisation of a β-cell specific *Mcl-1* knockout mouse strain, islet isolation, culture and glucose-stimulated insulin secretion and cell lines utilized

The human β-cell line EndoCβH1 and the rat insulinoma cell line INS-1E were cultured as described (14). Human islets were isolated from 6 non-diabetic organ donors (age 74±3 years; BMI 25±1 kg/m^2, insulin positive cells 63±8%) in Pisa, Italy, with the approval of the local human research ethics committee. These islets were cultured and treated as described (16).

Conditional *Mcl-1* knockout mice were generated as described (17). *Mcl-1*$^{fl/fl}$ mice were crossed with *RIP-Cre* transgenic mice (18) to generate a β-cell specific *Mcl-1* knockout mouse (*βMcl-1*KO) line. Both lines are on the C57BL/6 genetic background and wild type (WT) littermates were used as controls. *βMcl-1*KO mice were born at the expected normal Mendelian ratio. The non-fasted-glycaemia and body weight were followed in male and female *βMcl-1*KO mice and their respective WT littermates from 6-24 weeks (data not shown, and Suppl. Fig. 2). An intra-peritoneal glucose tolerance test (ipGTT) was performed in these animals at 12 and 24 weeks of age. Mice were injected with 2g/kg body weight glucose after 6 h of fasting. At 24 weeks, mice were sacrificed and their pancreas collected for measuring the total pancreatic insulin content

(19) or for immunofluorescence analysis (see below). Mice were housed and handled according to the Belgian Regulations for Animal Care and with permission from the local Ethic Committee.

For *ex vivo* experiments, mouse islets were isolated and cultured as described (20). Glucose-stimulated insulin secretion (GSIS) was performed in freshly isolated islets (19; 21). Insulin was quantified using the Ultra Sensitive Mouse Insulin ELISA Kit (Crystal Chem, Downers Grove, USA). The GSIS experiments were performed and measured in triplicates.

Multiple low-dose streptozotocin treatment

Non-fasted male mice aged 7-8 weeks were injected i.p. for 5 consecutive days with either 42.5 mg/kg body weight streptozotocin (Sigma-Aldrich, Belgium) dissolved in citrate buffer (100 mM pH $\leq$ 4.5, made freshly) or citrate buffer alone. Blood glucose levels were measured on days -3, 1, 2, 3, 4, 5 pre- and post-injection and later weekly during 10 weeks after the last injection in non-fasting conditions using a glucometer (Accu-Chek, Roche, Switzerland) (22). Hyperglycaemia was defined as non-fasting blood glucose levels >200 mg/dL in two sequential measurements. At the end of the experiment, the animals were sacrificed and the pancreas collected for histological analysis or for measuring the insulin content.

Immunofluorescence

Pancreatic tissues were collected and fixed overnight in 4% formaldehyde (BDH-Prolabo, Radnor, USA). Subsequently, the tissues were embedded in paraffin and at least 3 different sections were stained for analysis as described (23). Antibodies used are listed in Suppl. Table 2. Semi-quantitative analysis of insulin and glucagon staining was performed by analysing at least 3 different pancreas sections of 3 different animals per genotype, with a minimum of 15 islets examined per animal.

RNA interference, transient transfection, infection with recombinant adenovirus and site-directed mutagenesis

The small interfering (si)RNAs (30 nmol/L) used are listed in Suppl. Table 3 and transfections were performed as described (13; 16; 24). MCL-1 overexpression was achieved by transient transfection with a plasmid encoding rat MCL-1 (16) or by adenoviral infection (11). Control adenoviruses encoding luciferase or β-galactosidase were obtained from SIRION Biotech (Martinsried, Germany). The expression vector for FLAG-tagged rat MCL-1 (Agilent Technologies, Santa Clara, USA) was kindly provided by Prof. Eminy Lee (Institute of Biomedical Science of Taipei, Taiwan). Sequences encoding non-tagged rat MCL-1 were cloned into the pExpress plasmid (Express Genomics, MD, USA). The constructs encoding the phosphorylation site mutants of rat MCL-1 were generated using the Q5-Site directed mutagenesis kit (NEB, Ipswich, USA) using the WT rat Flag-MCL-1 vector as a template.

Assessment of cell viability

The percentages of viable, apoptotic and necrotic cells were determined using the DNA-binding dyes Propidium Iodide (PI, 5 µg/mL, Sigma-Aldrich) and Hoechst 33342 (HO, 5 µg/mL, Sigma-Aldrich), as described (11). In all experiments, the numbers of necrotic cells were low (between 1.8-2.1%) and did not change between the different conditions. For mouse islets, the percentages of dead cells were evaluated in a minimum of 10 islets per condition. All assessments were performed by two independent researchers one of whom was unaware of the identity of the samples.

Quantitative RT-PCR, immunoprecipitation and Western blot analysis

Poly(A)$^+$mRNA was isolated and reverse-transcribed as described (16). The real-time PCR amplification reaction was performed using SYBR Green and compared with a standard curve (25). All primers used are listed in Suppl. Table 3.

For total cellular extracts, cells were lysed in Laemmli buffer and for immunoprecipitation 1x RIPA buffer and the lysates were processed as described in (26). Western blot analysis was performed as described (11). The antibodies used are listed in the Suppl. Table 2. Images were acquired by Chemidoc (BioRad, Temse, Belgium) and analysed using ImageJ 1.49 software (27).

Flow cytometric analysis (FACS)

Single mouse islet cell preparations were obtained as described (20). To exclude dead cells, cells were stained using the LIVE/DEAD fixable dead cell stain kit (Life Technologies, Belgium). APC-anti-human CD4 (mouse, clone RPA-T4) antibody was used to assess *Mcl-1* gene deletion (28; 29). Cells were acquired on a FACSCanto II flow cytometer (BD Biosciences) and the data were analyzed using the FlowJo software (TreeStar, Ashland, OR) (29). The sorting of β-cell enriched cell populations was performed as described (30).

Statistical Analysis

Data are presented as means ± SEM. Comparisons were performed by two-tailed paired Student's *t*-test or by ANOVA followed by paired *t*-test with Bonferroni correction for multiple comparisons. A p value of <0.05 was considered as statistically significant.

RESULTS

Pro-inflammatory cytokines decrease MCL-1 protein expression in human pancreatic β-cells contributing to apoptosis.

Exposure of human EndoCβH1 cells to IL-1β+IFN-γ or TNF+IFN-γ for 16h induced significant increase in β-cell apoptosis that was further slightly increased at 24h (Suppl. 1a). By 24h, these inflammatory cytokines also caused a significant reduction of the expression of MCL-1 protein (up to 50%) in EndoCβH1 cells (Fig. 1a). We next exposed EndoCβH1 cells to different concentrations of cytokines for 24h. In all conditions, a significant reduction of MCL-1 expression (Fig. 1b) and increased apoptosis of EndoCβH1 cells (Figs. 1c-d) was observed. Moreover, knockdown of *Mcl-1* further increased the killing of EndoCβH1 cells induced by these cytokine combinations (Figs. 1c-d and Suppl. Fig. 1b-c). A second siRNA confirmed the potentiating effect of *Mcl-1* knockdown on cytokine-mediated apoptosis of EndoCβH1 cells (Suppl. Figs. 1b-d). In converse experiments, overexpression of rat MCL-1 using an adenovirus system (Ad-MCL-1), diminished cytokine-mediated apoptosis in both EndoCβH1 cells and primary human islet cells (Figs. 1e-f and Suppl. Figs. 1e-f).

MCL-1 depletion *in vivo* sensitises mouse islet cells to inflammatory cytokine-mediated death and renders mice more susceptible to diabetes

To explore the role of MCL-1 in islet cells *in vivo,* we generated a β-cell specific *Mcl-1* knockout mouse strain (*βMcl-1*KO). The expression of MCL-1 protein in islets was significantly reduced in *βMcl-1*KO mice as determined by Western blot analysis (Fig. 2a). In *βMcl-1*KO mice, a human CD4 reporter is subjugated to *Mcl-1* promoter/enhancer elements as described in (17). Therefore, β-cells in which $Mcl\text{-}1^{fl}$ has been deleted expressed the hCD4 protein that can be

detected by FACS using fluorochrome-labeled anti-human-CD4 antibodies. We observed that 91.3±0.5% of the β-cell enriched population from *βMcl-1KO* mice expressed the hCD4 protein, while only 3.9±0.3% of the β-cell depleted population expressed this marker (Fig. 2b). As expected, hCD4 expression was undetectable in β cells from WT mice (Fig. 2b). These results indicate an efficient recombination process and *Mcl-1*^{fl} deletion in *βMcl-1*KO mice.

β-cell death induced by IL-1β+IFN-γ or TNF+IFN-γ was exacerbated in islets from *βMcl*-1KO mice (Figs. 2c-d). Neither mRNA nor protein expression of BCL-2 and BCL-XL were altered in islets from *βMcl-1*KO mice (Figs. 2e-h). The *βMcl-1*KO mice were born at the expected Mendelian ratio and showed no obvious abnormalities up to 24 weeks (data not shown). Intra-peritoneal glucose tolerance tests (ipGTT) showed no difference between WT and *βMcl-1*KO mice (Suppl. Figs 2a-d). There were also no differences in fed blood glucose or body weight between WT and *βMcl-1*KO mice (Suppl. Figs 2e-f). Moreover, the total insulin content of the pancreas, islet morphology and β-cell response to glucose were normal in the *βMcl-1*KO mice (Suppl. Figs. 2g-k).

We next evaluated whether *βMcl-1*KO mice are more susceptible to diabetes induced by MLDSTZ, a treatment that induces a combined toxic autoimmune form of diabetes in mice (31; 32). As expected, both WT and *βMcl-1*KO mice developed hyperglycemia 10 days after the last injection of streptozotocin (Fig. 3a). The pancreatic insulin content was decreased by 60-90% in animals of both genotypes as compared to control buffer injected mice (Fig. 3c-d). Interestingly, MLDSTZ-induced hyperglycaemia was more severe in *βMcl-1*KO mice, with a 2-fold increase in the AUC calculated based on the glycaemic values as compared to WT littermates (Figs. 3a-b). In line with this, the insulin content of pancreata from *βMcl-1*KO mice was >50% lower than in WT mice after MLDSTZ treatment (Fig. 3c). Analysis of the pancreatic sections of both

*βMcl-1*KO and WT mice showed a clear decrease in the numbers of islets as well as insulin staining in the MLDSTZ treated animals of both genotypes compared to the vehicle injected mice (Fig. 3e). Islets from the MLDSTZ treated *βMcl-1*KO mice displayed reduced insulin staining compared to their WT counterparts (Fig. 3e and Suppl. Fig. 2k). In line with these observations, an increased percentage of α-cells was observed in MLDSTZ treated mice as compared to their vehicle treated counterparts (Fig. 3e and Suppl. Fig. 2l). Collectively, these results demonstrate that β-cells from *βMcl-1*KO mice are abnormally sensitive to stress.

GSK3β is critical for cytokine-mediated MCL-1 degradation

We have previously shown that the cytokine-mediated MCL-1 protein decrease in rat β-cells is a post-transcriptional process since these cells actually displayed increased *Mcl-1* mRNA levels (11). We have now made similar observations in human β-cells, since cytokines cause an increase in *MCL-1* mRNA expression in EndoCβH1 cells (Suppl. Fig. 3a). Studies in other cell types showed that MCL-1 protein stability can be regulated through phosphorylation by GSK3β, which primes MCL-1 for ubiquitination and proteasomal degradation (33). Inhibition of GSK3 using specific compounds did not affect MCL-1 protein expression under basal condition but it diminished the cytokine-mediated reduction in MCL-1 protein expression (Fig. 4a). β-catenin, a known target of GSK3 kinase, was reported to be modulated by the GSK3 inhibitors. Inhibition of GSK3β activity induced a significant protection from cytokine-induced cell death in both rat INS-1E cells and human EndoCβH1 cells (Figs. 4b-c).

GSK3β-targeted phosphorylation sites are conserved between human and rat MCL-1 (Fig. 5a) (33). We therefore generated expression vectors for rat phosphorylation site mutant MCL-1

proteins in which serine 139 or 142, or threonine 143 were substituted for by the phospho-null residue alanine. Treatment with cytokines downregulated the levels of both the overexpressed and exogenous WT MCL-1 protein with similar kinetics as the endogenous MCL-1 protein in INS-1E cells (Suppl. Fig. 3b). The expression levels of all MCL-1 protein forms were comparable in untreated cells (Suppl. Fig. 3c). The T143A mutation diminished cytokine-mediated decrease in MCL-1 protein expression at 16h but not at 24h (Fig. 5b). Conversely, the S139A mutation resulted in more substantial protection against IL-1β+IFN-γ-induced MCL-1 degradation (Fig. 5c). Finally, the S142A mutation did not affect MCL-1 protein turnover (Fig. 5d). A significant decrease in cytokine-mediated caspase-3 activation was observed in INS-1 cells overexpressing the S139A mutant form of MCL-1 (Figs. 5b-e). These results show that GSK3β mediated phosphorylation controls the levels of MCL-1 protein in cytokine treated pancreatic β-cells and thereby controls their survival.

MCL-1 is ubiquitinated in response to treatment with IL-1β plus IFN-γ and this process is regulated by E3-ligases and the de-ubiquitinase USP9x.

Exposure of INS-1E cells to IL-1β+IFN-γ did not affect the general protein ubiquitination pattern (Fig. 6a, left - input), but it increased the ubiquitination of over-expressed WT-FLAG-MCL-1 (Fig. 6a, right - anti-FLAG). In certain tumour cells, MCL-1 was shown to be ubiquitinated by the E3 ubiquitin-ligases, F-box and WD repeat domain-containing 7 (FBW7), beta-transducin repeat containing protein (βTrCP) and the MCL-1 ubiquitin ligase (MULE) (34). We found that FBW7 was downregulated in β-cells upon treatment with IL-1β+IFN-γ (14), and conversely, the levels of MULE and βTrCP were increased under these conditions (Figs. 6b-c). Knockdown of FBW7 with a previously validated small interfering RNA (siRNA) (14) increased MCL-1

expression under basal conditions, but had no impact on the cytokine-mediated decrease of this protein (Fig. 6d). Conversely, knockdown of MULE or βTrCP, using two different siRNAs for each target, did not alter MCL-1 protein levels under basal conditions, but it substantially reduced the cytokine-mediated loss of MCL-1 in INS-1E cells (Figs. 6e-f, Suppl. Figs. 4a-d).

The ubiquitin-specific peptidase 9 X-linked (USP9x) was shown to de-ubiquitinate MCL-1 in certain tumour cells, thereby protecting MCL-1 from proteasomal degradation (35). Treatment with IL-1β+IFN-γ decreased the expression of USP9x in INS-1E cells (Fig. 6g) and knockdown of USP9x using two different siRNAs potentiated the IL-1β+IFN-γ-mediated decrease in MCL-1 levels (Fig. 6h and Suppl. Figs. 4e-f). These results show that pro-inflammatory cytokines increase the expression of the E3 ligases βTrCP and MULE but decrease the expression of the de-ubiqutinase, USP9x. These processes together conspire to cause a reduction in MCL-1 protein.

DISCUSSION

MCL-1 is an anti-apoptotic member of the BCL-2 protein family that protects pancreatic cells against apoptosis by sequestering the multi-BH domain pro-apoptotic BAX/BAK proteins, and the pro-apoptotic BH3-only proteins, such as BIM and PUMA (7; 33). We have previously shown that a variety of cytotoxic stimuli, such as, pro-inflammatory cytokines, the ER stressor thapsigargin, the saturated acid palmitate and the viral mimetic double-stranded RNA, promote apoptosis by decreasing MCL-1 protein levels in rat β-cells (7; 11). We observed here that inflammatory cytokines also decrease MCL-1 protein expression in human β-cells and that this contributes to the apoptosis of these cells. Interestingly, dose response experiments indicated that relatively low levels of cytokines were already able to decrease MCL-1 levels and induce death of EndoCβH1 cells. These results are in line with a recent report, revealing decreased expression of MCL-1 in islets from T1D patients infected with diabetogenic enterovirus (12). Collectively, these findings suggest that decreased levels of MCL-1 in β-cells may contribute to the development of diabetes.

We report here that MCL-1 overexpression partially protects human β-cell against the pro-apoptotic effect of pro-inflammatory cytokines. To evaluate the protective role of MCL-1 in immune-mediated β-cell death *in vivo,* we developed a β-cell specific *Mcl-1* KO mouse strain. *βMcl-1*KO mice were born at the expected Mendelian frequency and showed no obvious metabolic abnormalities even in adulthood. This is remarkable, because loss of MCL-1 in other essential cell types, such as neurons, cardiomyocytes or haematopoietic stem/progenitor cells, causes death of mice (36-39). It is therefore possible that during development β-cells are less dependent on MCL-1 than these other cell types, suggesting that the survival of β-cells may be

safeguarded by other pro-survival BCL-2 family members (e.g. BCL-XL) or that several of these pro-survival proteins function in these cells in an overlapping manner.

In agreement with findings from *Mcl-1* gene knockdown studies in rodent and human β-cells ((11) and present data), islets from the *βMcl-1*KO mice were abnormally susceptible to cell death induced by both IL-1β+IFN-γ or TNF+IFN-γ treatment. MLDSTZ treatment induces a slow and progressive decrease in insulin levels due to direct toxicity and islet inflammation with consequent β-cell killing (31; 32). The development of diabetes in our experiments followed the usual time course in this model, with hyperglycaemia appearing 10 days after the end of streptozotocin treatment, indicating that the disease was mainly due to islet inflammation. Interestingly, MLDSTZ treatment induced a more pronounced hyperglycaemia in the *βMcl-1*KO mice compared to their WT littermates, as reflected by a 2-fold increase in the AUC calculated based on the glycaemic levels. In line with these data, there was a >50% decrease in insulin content in *βMcl-1*KO mice as compared to their WT littermates. Moreover, histological analysis of the pancreas showed a reduced percentage of insulin positive cells and an increased percentage of glucagon positive cells in the *βMcl-1*KO islets. The increased glucagon staining probably reflects the stronger depletion of insulin positive cells in the KO islets. These results indicate that MLDSTZ treatment causes increased β-cell destruction in the *βMcl-1*KO mice. This could be due to increased mononuclear cell infiltration in *βMcl-1*KO mice, since islets from these mice are probably more susceptible to STZ- and immune-induced cell death than wild type islets, and this could lead to increased inflammation (40). Overall, our results establish the crucial role for MCL-1 in protecting mouse as well as human β-cells from apoptosis *in vitro* and during diabetes development in mice *in vivo*.

Our next aim was to unravel the regulatory mechanisms that drive inflammatory cytokine mediated MCL-1 downregulation in pancreatic β-cells. Due to its short half-life (~30 min; compared to ~20 h for BCL-XL and BCL-2), MCL-1 is disproportionally susceptible to alterations in protein translation (33). MCL-1 is structurally unique among other anti-apoptotic proteins of the BCL-2 family, since it contains an N-terminal domain with several phospho-degron motives that are associated with its rapid turnover (33; 34). JNK-mediated phosphorylation decreases MCL-1 protein stability, a process that can be prevented by JNK inhibitors (11). Phosphorylation by GSK3β can also promote MCL-1 protein degradation, at least in cancer cells (33). We have now found that inhibition of GSK3β, using two specific compounds, diminishes IL-1β+IFN-γ mediated MCL-1 protein degradation. This was accompanied by a significant protection against cytokine-induced apoptosis in both rat and, importantly, human β-cells.

We hypothesised that mutations of the GSK-3β-targeted phospho-degrons might disrupt MCL-1 phosphorylation and thereby increase MCL-1 protein stability. In rat MCL-1, threonine 143 (corresponding to Thr163 in human MCL-1) acts as a critical primary phosphorylation site that then primes MCL-1 for subsequent phosphorylation at other sites, as shown in different cell types (41; 42). Surprisingly, in our studies the T143A mutation only delayed cytokine mediated MCL-1 degradation. This suggests that phosphorylation of T143 contributes, but is not an absolute prerequisite for GSK3β-mediated phosphorylation of other sites in MCL-1 and its degradation in INS-1E cells (33; 34). This indicates that cell type specific differences exist in the post-translational modifications of MCL-1 and the control of its turnover. Furthermore, our studies revealed that serine 139 in rat MCL-1 (corresponding to S159 in human MCL-1) is critical for MCL-1 degradation in INS-1E cells. Indeed, the S159A mutation substantially

protected MCL-1 against cytokine-induced degradation in INS-1E cells and this decreased caspase-3 activation, indicating protection against apoptosis. The S159 residue was shown to be phosphorylated only by GSK3β, reducing the anti-apoptotic function of MCL-1 by priming it for ubiquitination and proteasomal degradation (33; 34). Accordingly, we found that treatment with IL-1β+IFN-γ induces prominent ubiquitination of MCL-1 in INS-1E cells.

Several E3 ligases, including MULE, βTrCP and FBW7, contribute to the ubiquitination-mediated proteasomal degradation of MCL-1 in cancer cells after phosphorylation by GSK3β (34). Interestingly, we observed that pro-inflammatory cytokines modulate the mRNA expression of these three E3 ligases in INS-1E cells. While Mule and βTrCP are upregulated, FBW7 expression is downregulated after exposure to IL-1β+IFN-γ (Fig. 7). In HeLa cells MULE was shown to ubiquitinate MCL-1 and thereby prime it for proteasomal degradation whereas, conversely, knockdown of MULE was found to increase MCL-1 protein levels in sarcoma cells and thereby protected them from apoptosis induced by DNA damage (34). In A293T cells, overexpression of βTrCP induced MCL-1 ubiquitination, followed by a decrease in its levels. The opposite was seen when βTrCP expression was silenced (34). In agreement with these reports, we observed that knockdown of both MULE and βTrCP increased the levels of MCL-1 protein even when the INS-1E cells were exposed to IL-1β+IFN-γ. This suggests that pro-inflammatory cytokine-induced MCL-1 degradation depends on ubiquitination mediated by these E3 ligases. Surprisingly, knockdown of FBW7 in INS-1E cells increased MCL-1 expression only under control (no treatment) conditions, suggesting that this E3 ligase regulates MCL-1 steady-state protein levels but has no role in MCL-1 degradation induced by cytotoxic stressors, at least in this cell type. This may be explained by the fact that depletion of this E3 ligase enhances NF-

κB-mediated NO generation (14), which has previously been shown to induce ER stress and a consequent decrease in MCL-1 (Fig. 7) (11).

Besides the effects of E3 ligases, MCL-1 turnover is also affected by the opposing action of the de-ubiquitinase, USP9x. USP9x antagonises K48-linked poly-ubiquitination and thereby stabilises the MCL-1 protein, allowing it to inhibit apoptosis (35). Interestingly, exposure to pro-inflammatory cytokines decreased expression of USP9x in INS-1E cells, while knockdown of USP9x significantly decreased MCL-1 expression in both untreated and cytokine-treated INS-1E cells. Collectively, these findings suggest that the de-ubiquitinase USP9x contributes to MCL-1 stabilisation by antagonising its K48-linked poly-ubiquitination and thereby functions as an inhibitor of apoptosis in β-cells (Fig. 7).

In conclusion, the data presented here provide evidence that MCL-1 exerts a critical anti-apoptotic role in human β-cells *in vitro*, and its deficiency affects diabetes development in mice. Moreover, we clarified the mechanisms that regulate MCL-1 protein turnover in rat β-cells when exposed to a pro-inflammatory milieu (Fig. 7). Prevention of MCL-1 downregulation in β-cells might be achieved via multiple ways: inhibition of GSK3β kinase, mutation of critical residues in the MCL-1 phosphodegron motives or modulation of ubiquitin editing enzymes, such as overexpression of the deubiquitinase USP9x. This information might serve as a basis for development of new strategies to prevent β-cell death in T1D.

ACKNOWLEDGEMENTS

We thank S. Mertens for expert technical assistance, as well as, A. Musuaya and M. Pangerl; Prof. Rudi Beyaert (VIB Gent, Belgium) and his team for helpful advice regarding ubiquitination/immunoprecipition and Dr Philippe Bouillet (WEHI) for *Mcl-1* gene targeted mice. Work in the A.K.C. group was supported by the Juvenile Diabetes Research Foundation (JDRF-New York-USA; 1-2011-589), Actions de Recherche Concertées de la Communauté Française (ARC – Belgium; 20063), National Funds from Scientific Research (FNRS, Belgium; T.0107.16). The research of D.L.E. was supported by the FNRS (T.0036.13). D.L.E. and P.M. received funding from the European Union's Horizon 2020 research and innovation programme project T2DSystems, under grant agreement No 667191, and from the Innovative Medicines Initiative 2 Joint Undertaking under grant agreement No 115797 (INNODIA). This Joint Undertaking receives support from the Union's Horizon 2020 research and innovation programme and "EFPIA", 'JDRF" and "The Leona M. and Harry B. Helmsley Charitable Trust". NVM was a recipient of a PhD scholarship from the São Paulo Research Foundation (FAPESP-2015/01237-0). The research of A.S. group was supported by the National Health and Medical Research Council (NHMRC; program grant no. 1016701) and the Leukemia & Lymphoma Society of America (Specialized Center of Research [SCOR]; 7001-13). A.S. is a recipient of a NHMRC Senior Principal Research Fellow [SPRF] Fellowship (NHMRC;-1020363).

AUTHOR CONTRIBUTION

K.M., A.K.C., D.L.E., A.S. and N.V.M. contributed to the study concept and design, analysis and interpretation of the data. K.M., N.V.M, N.P., M.F. and V.D. contributed to the acquisition of the data. P.M. and A.S. contributed reagents/materials/analytical tools. K.M., A.K.C, N.V.M.,

A.S. and D.L.E. wrote/edited the manuscript. A.K.C. is responsible for its content. All authors revised the article and approved the final version.

CONFLICT OF INTEREST

The authors declare no conflict of interest.

REFERENCES:

1. Eizirik DL, Colli ML, Ortis F: The role of inflammation in insulitis and beta-cell loss in type 1 diabetes. Nat Rev Endocrinol 2009;5:219-226
2. Eizirik DL, Sammeth M, Bouckenooghe T, Bottu G, Sisino G, Igoillo-Esteve M, Ortis F, Santin I, Colli ML, Barthson J, Bouwens L, Hughes L, Gregory L, Lunter G, Marselli L, Marchetti P, McCarthy MI, Cnop M: The human pancreatic islet transcriptome: expression of candidate genes for type 1 diabetes and the impact of pro-inflammatory cytokines. PLoS genetics 2012;8:e1002552
3. Lundberg M, Krogvold L, Kuric E, Dahl-Jorgensen K, Skog O: Expression of Interferon-Stimulated Genes in Insulitic Pancreatic Islets of Patients Recently Diagnosed with Type 1 Diabetes. Diabetes 2016; 65: 3104-3110.
4. Meyerovich K, Ortis F, Allagnat F, Cardozo AK: Endoplasmic reticulum stress and the unfolded protein response in pancreatic islet inflammation. J Mol Endocrinol 2016;57:R1-R17
5. Gurzov EN, Eizirik DL: Bcl-2 proteins in diabetes: mitochondrial pathways of beta-cell death and dysfunction. Trends Cell Biol 2011;21:424-431
6. Youle RJ, Strasser A: The BCL-2 protein family: opposing activities that mediate cell death. Nat Rev Mol Cell Biol 2008;9:47-59
7. Colli ML, Nogueira TC, Allagnat F, Cunha DA, Gurzov EN, Cardozo AK, Roivainen M, Op de Beeck A, Eizirik DL: Exposure to the viral by-product dsRNA or Coxsackievirus B5 triggers pancreatic beta cell apoptosis via a Bim / Mcl-1 imbalance. PLoS Pathog 2011;7:e1002267
8. Puthalakath H, O'Reilly LA, Gunn P, Lee L, Kelly PN, Huntington ND, Hughes PD, Michalak EM, McKimm-Breschkin J, Motoyama N, Gotoh T, Akira S, Bouillet P, Strasser A: ER stress triggers apoptosis by activating BH3-only protein Bim. Cell 2007;129:1337-1349
9. Gurzov EN, Germano CM, Cunha DA, Ortis F, Vanderwinden JM, Marchetti P, Zhang L, Eizirik DL: Puma activation contributes to pancreatic beta cell apoptosis induced by pro-inflammatory cytokines and endoplasmic reticulum stress. J Biol Chem 2010;258:19910-19920
10. Roggli E, Gattesco S, Caille D, Briet C, Boitard C, Meda P, Regazzi R: Changes in MicroRNA Expression Contribute to Pancreatic beta-Cell Dysfunction in Prediabetic NOD Mice. Diabetes 2012;61:1742-1751
11. Allagnat F, Cunha D, Moore F, Vanderwinden JM, Eizirik DL, Cardozo AK: Mcl-1 downregulation by pro-inflammatory cytokines and palmitate is an early event contributing to beta-cell apoptosis. Cell Death Differ 2011;18:328-337
12. Richardson SJ, Leete P, Bone AJ, Foulis AK, Morgan NG: Expression of the enteroviral capsid protein VP1 in the islet cells of patients with type 1 diabetes is associated with induction of protein kinase R and downregulation of Mcl-1. Diabetologia 2013;56:185-193
13. Grieco FA, Moore F, Vigneron F, Santin I, Villate O, Marselli L, Rondas D, Korf H, Overbergh L, Dotta F, Marchetti P, Mathieu C, Eizirik DL: IL-17A increases the expression of proinflammatory chemokines in human pancreatic islets. Diabetologia 2014;57:502-511
14. Meyerovich K, Fukaya M, Terra LF, Ortis F, Eizirik DL, Cardozo AK: The non-canonical NF-kappaB pathway is induced by cytokines in pancreatic beta cells and contributes to cell death and proinflammatory responses in vitro. Diabetologia 2016;59:512-521
15. Cardozo AK, Ortis F, Storling J, Feng YM, Rasschaert J, Tonnesen M, Van Eylen F, Mandrup-Poulsen T, Herchuelz A, Eizirik DL: Cytokines downregulate the sarcoendoplasmic reticulum pump Ca2+ ATPase 2b and deplete endoplasmic reticulum Ca2+, leading to induction of endoplasmic reticulum stress in pancreatic beta-cells. Diabetes 2005;54:452-461
16. Allagnat F, Fukaya M, Nogueira TC, Delaroche D, Welsh N, Marselli L, Marchetti P, Haefliger JA, Eizirik DL, Cardozo AK: C/EBP homologous protein contributes to cytokine-induced pro-inflammatory responses and apoptosis in beta-cells. Cell Death Differ 2012;19:1836-1846
17. Grabow S, Delbridge AR, Aubrey BJ, Vandenberg CJ, Strasser A: Loss of a Single Mcl-1 Allele Inhibits MYC-Driven Lymphomagenesis by Sensitizing Pro-B Cells to Apoptosis. Cell reports 2016;14:2337-2347

18. Schaffer AE, Yang AJ, Thorel F, Herrera PL, Sander M: Transgenic overexpression of the transcription factor Nkx6.1 in beta-cells of mice does not increase beta-cell proliferation, beta-cell mass, or improve glucose clearance. Mol Endocrinol 2011;25:1904-1914
19. Hennige AM, Burks DJ, Ozcan U, Kulkarni RN, Ye J, Park S, Schubert M, Fisher TL, Dow MA, Leshan R, Zakaria M, Mossa-Basha M, White MF: Upregulation of insulin receptor substrate-2 in pancreatic beta cells prevents diabetes. J Clin Invest 2003;112:1521-1532
20. Fukaya M, Brorsson CA, Meyerovich K, Catrysse L, Delaroche D, Vanzela EC, Ortis F, Beyaert R, Nielsen LB, Andersen ML, Mortensen HB, Pociot F, van Loo G, Storling J, Cardozo AK: A20 Inhibits beta-Cell Apoptosis by Multiple Mechanisms and Predicts Residual beta-Cell Function in Type 1 Diabetes. Mol Endocrinol 2016;30:48-61
21. Wagner AM, Cloos P, Bergholdt R, Eising S, Brorsson C, Stalhut M, Christgau S, Nerup J, Pociot F: Posttranslational Protein Modifications in Type 1 Diabetes - Genetic Studies with PCMT1, the Repair Enzyme Protein Isoaspartate Methyltransferase (PIMT) Encoding Gene. Rev Diabet Stud 2008;5:225-231
22. Catrysse L, Fukaya M, Sze M, Meyerovich K, Beyaert R, Cardozo AK, van Loo G: A20 deficiency sensitizes pancreatic beta cells to cytokine-induced apoptosis in vitro but does not influence type 1 diabetes development in vivo. Cell Death Dis 2015;6:e1918
23. Brozzi F, Gerlo S, Grieco FA, Nardelli TR, Lievens S, Gysemans C, Marselli L, Marchetti P, Mathieu C, Tavernier J, Eizirik DL: A combined "omics" approach identifies N-Myc interactor as a novel cytokine-induced regulator of IRE1 protein and c-Jun N-terminal kinase in pancreatic beta cells. J Biol Chem 2014;289:20677-20693
24. Moore F, Cunha DA, Mulder H, Eizirik DL: Use of RNA interference to investigate cytokine signal transduction in pancreatic beta cells. Methods in molecular biology 2012;820:179-194
25. Rasschaert J, Ladriere L, Urbain M, Dogusan Z, Katabua B, Sato S, Akira S, Gysemans C, Mathieu C, Eizirik DL: Toll-like Receptor 3 and STAT-1 contribute to double-stranded RNA+ interferon-gamma-induced apoptosis in primary pancreatic beta-cells. J Biol Chem 2005;280:33984-33991
26. Shoda H, Fujio K, Shibuya M, Okamura T, Sumitomo S, Okamoto A, Sawada T, Yamamoto K: Detection of autoantibodies to citrullinated BiP in rheumatoid arthritis patients and pro-inflammatory role of citrullinated BiP in collagen-induced arthritis. Arthritis research & therapy 2011;13:R191
27. Schneider CA, Rasband WS, Eliceiri KW: NIH Image to ImageJ: 25 years of image analysis. Nat Methods 2012;9:671-675
28. Kelly GL, Grabow S, Glaser SP, Fitzsimmons L, Aubrey BJ, Okamoto T, Valente LJ, Robati M, Tai L, Fairlie WD, Lee EF, Lindstrom MS, Wiman KG, Huang DC, Bouillet P, Rowe M, Rickinson AB, Herold MJ, Strasser A: Targeting of MCL-1 kills MYC-driven mouse and human lymphomas even when they bear mutations in p53. Genes Dev 2014;28:58-70
29. Wyndham-Thomas C, Corbiere V, Dirix V, Smits K, Domont F, Libin M, Loyens M, Locht C, Mascart F: Key role of effector memory CD4+ T lymphocytes in a short-incubation heparin-binding hemagglutinin gamma interferon release assay for the detection of latent tuberculosis. Clin Vaccine Immunol 2014;21:321-328
30. Marroqui L, Masini M, Merino B, Grieco FA, Millard I, Dubois C, Quesada I, Marchetti P, Cnop M, Eizirik DL: Pancreatic alpha Cells are Resistant to Metabolic Stress-induced Apoptosis in Type 2 Diabetes. EBioMedicine 2015;2:378-385
31. McEvoy RC, Andersson J, Sandler S, Hellerstrom C: Multiple low-dose streptozotocin-induced diabetes in the mouse. Evidence for stimulation of a cytotoxic cellular immune response against an insulin-producing beta cell line. J Clin Invest 1984;74:715-722
32. Paik SG, Fleischer N, Shin SI: Insulin-dependent diabetes mellitus induced by subdiabetogenic doses of streptozotocin: obligatory role of cell-mediated autoimmune processes. Proc Natl Acad Sci U S A 1980;77:6129-6133
33. Thomas LW, Lam C, Edwards SW: Mcl-1; the molecular regulation of protein function. FEBS Lett 2010;584:2981-2989
34. Mojsa B, Lassot I, Desagher S: Mcl-1 ubiquitination: unique regulation of an essential survival protein. Cells 2014;3:418-437

35. Schwickart M, Huang X, Lill JR, Liu J, Ferrando R, French DM, Maecker H, O'Rourke K, Bazan F, Eastham-Anderson J, Yue P, Dornan D, Huang DC, Dixit VM: Deubiquitinase USP9X stabilizes MCL1 and promotes tumour cell survival. Nature 2010;463:103-107
36. Opferman JT, Iwasaki H, Ong CC, Suh H, Mizuno S, Akashi K, Korsmeyer SJ: Obligate role of anti-apoptotic MCL-1 in the survival of hematopoietic stem cells. Science 2005;307:1101-1104
37. Arbour N, Vanderluit JL, Le Grand JN, Jahani-Asl A, Ruzhynsky VA, Cheung EC, Kelly MA, MacKenzie AE, Park DS, Opferman JT, Slack RS: Mcl-1 is a key regulator of apoptosis during CNS development and after DNA damage. J Neurosci 2008;28:6068-6078
38. Wang X, Bathina M, Lynch J, Koss B, Calabrese C, Frase S, Schuetz JD, Rehg JE, Opferman JT: Deletion of MCL-1 causes lethal cardiac failure and mitochondrial dysfunction. Genes Dev 2013;27:1351-1364
39. Thomas RL, Roberts DJ, Kubli DA, Lee Y, Quinsay MN, Owens JB, Fischer KM, Sussman MA, Miyamoto S, Gustafsson AB: Loss of MCL-1 leads to impaired autophagy and rapid development of heart failure. Genes Dev 2013;27:1365-1377
40. Vanden Berghe T, Kaiser WJ, Bertrand MJ, Vandenabeele P: Molecular crosstalk between apoptosis, necroptosis, and survival signaling. Mol Cell Oncol 2015;2:e975093
41. Morel C, Carlson SM, White FM, Davis RJ: Mcl-1 integrates the opposing actions of signaling pathways that mediate survival and apoptosis. Mol Cell Biol 2009;29:3845-3852
42. Maurer U, Charvet C, Wagman AS, Dejardin E, Green DR: Glycogen synthase kinase-3 regulates mitochondrial outer membrane permeabilization and apoptosis by destabilization of MCL-1. Mol Cell 2006;21:749-760
43. Okamoto T, Coultas L, Metcalf D, van Delft MF, Glaser SP, Takiguchi M, Strasser A, Bouillet P, Adams JM, Huang DC: Enhanced stability of Mcl1, a prosurvival Bcl2 relative, blunts stress-induced apoptosis, causes male sterility, and promotes tumorigenesis. Proc Natl Acad Sci U S A 2014;111:261-266
44. Notredame C, Higgins DG, Heringa J: T-Coffee: A novel method for fast and accurate multiple sequence alignment. J Mol Biol 2000;302:205-217

FIGURE LEGENDS

Figure 1: ***Pro-inflammatory cytokines decrease MCL-1 protein expression in human pancreatic β-cells, contributing to apoptosis.*** **(a)** EndoCβH1 cells were treated with IL-1β (50 U/mL) + IFN-γ (1000 U/mL) or TNF (1000 U/mL) + IFN-γ (1000 U/mL) for 16 or 24 h and the expression of MCL-1 and α-tubulin (loading control) proteins were analysed by Western blotting (WB). A representative WB (left panel) and densitometric assessment of MCL-1 levels (right panel) are shown. *p<0.05, **p<0.01 *vs* untreated (0h) condition. **(b)** EndoCβH1 cells were treated with different concentrations of IL-1β+IFN-γ or TNF+IFN-γ for 24h, as indicated, and the expression of MCL-1 and α-tubulin (loading control) were analysed by WB. A representative WB (left panel) and densitometric assessment of MCL-1 levels (right panel) are shown. *p<0.05 *vs* untreated condition. **(c-d)** EndoCβH1 cells were transfected with siCTR (control siRNA) or *siMcl-1* RNA #2 and treated with different concentrations of IL-1β+IFN-γ (c) or TNF+IFN-γ (d) for 24h, as indicated. Cell viability was assessed by HO/PI staining. *p<0.05 *vs* siCTR under untreated condition; #p<0.05 *siMcl-1 vs* siCTR under the respective condition. **(e-f)** EndoCβH1 cells **(e)** or dispersed primary human islet cells **(f)** were transduced with a control adenovirus (AdCTR) or an adenovirus encoding rat MCL-1 (Ad-MCL-1) at multiplicity of infection (MOI) 10 and exposed to IL-1β (50 U/mL) +IFN-γ (1000 U/mL) or TNF (1000 U/mL) + IFN-γ (1000 U/mL) for 24h **(e)** or 48h **(f)** as indicated. *p<0.05, **p<0.01 *vs* AdCTR under untreated condition #p<0.05 Ad-MCL-1 *vs* AdCTR under the respective conditions. **(a-f)** Data represent mean ± SEM of 4-8 independent experiments.

Figure 2: ***Islet-cells from the βMcl-1KO mice are abnormally sensitive to pro-inflammatory cytokine-induced death.*** **(a)** Islets from *βMcl-1*KO (KO) and wild-type (WT) littermates were isolated and MCL-1 protein levels were examined. A representative WB (left panel) and densitometric assessment of MCL-1 levels (right panel) are shown. *p<0.05 *βMcl-1*KO *vs* WT. Of note, the upper MCL-1 band observed in islets from *βMcl-1*KO is due to the fact that during gene targeting (development of the *Mcl-1* floxed mice) inadvertently an in-frame sequence encoding a few amino acids at the N terminus was inserted (43) **(b)** Left panel: Representative FACS plot showing β-cell enriched and β-cell depleted cell populations selected based on their size and auto-fluorescence (30). Middle and right panels: representative FACS plot showing the expression of the human CD4 reporter on β-cell enriched and β-cell depleted populations from WT (grey) and *βMcl-1KO* mice (black). **(c-d)** Islets from *βMcl-1*KO mice or WT littermates were isolated and exposed to different concentrations of IL-1β+IFN-γ for 24h **(c)** or TNF+IFN-γ for 72h, as indicated **(d)**. Cell death was assessed by HO/PI staining. #p<0.05 *βMcl-1*KO *vs* WT under the respective condition. *p<0.05 WT cytokine *vs* WT untreated. **(e-h)** Mouse islets were isolated from *βMcl*KO and WT littermates and expression of BCL-XL and BCL-2 mRNA and protein were analysed by real time PCR **(e-g)** and Western blotting **(f-h)**, respectively. **(f-h)** A representative WB (left panel) and densitometric assessment of MCL-1 levels (right panel) are shown. Data represent mean ± SEM of 3-6 independent experiments.

Figure 3: ***Loss of MCL-1 sensitises mice to MLDSTZ-induced diabetes.*** **(a)** Male *βMcl-1*KO mice and WT littermates were injected with 42.5 mg/kg body weight of streptozotocin (STZ, n=11-13) or control buffer (Buffer, n=2-6) for 5 subsequent days. Fed glucose levels were measured at day -3, 1, 2, 3, 4, 5 of treatment and then at day 3, 10, 17, 24, 31, 38, 45, 52, 59 and

66 days after the last injection. *p<0.05 *βMcl-1*KO+MLDSTZ *vs* WT+MLDSTZ. **(b)** Quantitative analysis of the area under the curves (AUC) of the data from (**a,** MLDSTZ-treated animals**)** is shown. ***p<0.001 *βMcl-1*KO *vs* WT. **(c)** Total pancreatic insulin content was evaluated in MLDSTZ-treated animals at the end of the experiment. **p<0.05 *βMcl-1*KO *vs* WT. **(d)** Total pancreatic insulin content in *βMcl-1*KO and WT males from the control buffer-treated group. **(a-d)** Data represent mean ± SEM of 2-9 independent experiments. **(e)** Representative images of immunofluorescence staining for insulin (green), glucagon (red) and DAPI in islets from untreated (i.e. control) WT and *βMcl-1*KO mice (24-week old males) and mice of those genotypes after MLDSTZ treatment are shown. Scale bars, 2 μm- 20X.

Figure 4: ***GSK3β is required for cytokine-mediated MCL-1 protein degradation.*** **(a)** INS-1E cells were treated with DMSO (control) or the GSK3 inhibitors, SB or BIO, alone or in combination with treatment with IL-1β+IFN-γ for 16h. The expression of MCL-1, β-catenin and α-tubulin (loading control) proteins were analysed. A representative blot (left panel) and densitometric assessment of MCL-1 protein levels (right panel) are shown. **(b-c)** INS-1E **(b)** and EndoC-βH1 **(c)** cells were treated with DMSO (control) or the GSK3 inhibitors, SB or BIO, alone or in combination with pro-inflammatory cytokines for 16h **(b)** or 24h **(c)**, respectively, as indicated. Cell viability was assessed by HO/PI staining. **(a-c)** *p<0.05, **p<0.01, ***p<0.001 DMSO/cytokines *vs* DMSO/untreated condition; #p<0.05, ###p<0.001 *vs* DMSO/treated under respective condition. Data represent mean ± SEM of 4-5 independent experiments.

Figure 5: ***Identification of the amino acid residues in MCL-1 that are critical for its stability.*** **(a)** The amino acid sequences of human and rat MCL-1 were aligned by the t-coffee program (44). Identical and conserved amino acids are marked by black and grey boxes, respectively. **(b-**

e) Rat INS-1E cells were transfected with expression constructs encoding WT Flag-MCL-1 (WT) or the indicated Flag-MCL-1 mutants and exposed to IL-1β+IFN-γ for 0, 16 or 24h, as indicated. The expression levels of MCL-1, cleaved caspase-3 (a marker of apoptosis) and α-tubulin (loading control) proteins were analysed. **(b-d)** Representative WBs (upper panel) and densitometric assessments of WT and phospho-mutant MCL-1 proteins (lower panel) are shown. **(e)** A densitometric assessment of cleaved caspase-3 is shown. The levels of activated caspase-3 are represented as fold-change compared to WT cells at 0h. **(b-e)** *p<0.05 WT cytokine *vs* WT untreated (0h), #p<0.05, ##p<0.01, ###p<0.001 Flag-MCL-1 mutants *vs* WT MCL-1 under the respective conditions. Data represent mean ± SEM of 5 independent experiments.

Figure 6: ***Knockdown of MULE or βTrCP preserves MCL-1 protein levels upon pro-inflammatory cytokine exposure, whereas silencing of USP9x potentiates MCL-1 decrease.*** **(a)** INS-1E cells were transfected with expression constructs encoding WT Flag-MCL-1 and exposed to IL-1β+IFN-γ for 10h. Cells were lysed and extracts immunoprecipitated with Flag-tag antibody and immunoblotted for ubiquitin. A representative WB of at least 5 independent experiments is shown. **(b-c)** *Mule* **(b)** and *βTrCP* **(c)** mRNA expression in INS-1E cells exposed to IL-1β+IFN-γ for 16h *p<0.05 treated *vs* untreated condition. **(d-f)** INS-1E cells were transfected with siCTR (control siRNA), *siFbw7*, *siMule* (#1, #2) or *siβTrCP* (#1, #2) and treated with IL-1β+IFN-γ as indicated. The expression of MCL-1 and α-tubulin (loading control) proteins were analysed by Western blotting. A representative blot (upper panel) and densitometric assessment of MCL-1 protein levels (lower panel) are shown. **(g)** *USP9x* mRNA expression in INS-1E cells exposed to IL-1β+IFN-γ for 16h *p<0.05 treated *vs* untreated condition. **(h)** INS-1E cells were transfected with siCTR (control siRNA) or *siUSP9x* (#1, #2) and treated with IL-1β+IFN-γ for 16h. The expression of MCL-1 and α-tubulin (loading control)

proteins was analysed by Western blotting. A representative blot (upper panel) and densitometric assessment of MCL-1 (lower panel) are shown. **(d-f, h)** *p<0.05 siCTR cytokines *vs* siCTR under untreated condition; #p<0.05, ##p<0.01, ###p<0.001 *siUSP9x*, *siMULE* or *siβTrCP vs* siCTR under respective conditions. **(b-h)** Data represent mean ± SEM of 3-6 independent experiments.

Figure 7: ***The interplay of cytokine-induced signaling cascades and the ubiquitin-proteasome degradation pathway in the regulation of MCL-1 protein stability.***

Pro-inflammatory cytokines trigger activation of NF-κB transcription factors and the kinases, JNK and GSK3β. The IL-1β+IFN-γ-mediated decrease in FBW7 and increase in βTrCP contributes to activation of the NF-κB pathway (14). NF-κB-mediated NO generation contributes to MCL-1 decrease via induction of ER stress. Moreover, the NF-κB target gene encoded BH3-only protein PUMA inhibits MCL-1, thereby contributing to β-cell death (15). Phosphorylation by GSK3β (via the serine 139) primes MCL-1 for ubiquitination and degradation by the proteasome. This process is regulated by the E3 ligases, MULE and βTrCP, as well as by the de-ubiquitinase, USP9x. While treatment with IL-1β+IFN-γ induces the expression of the E3 ligases, MULE and βTrCP, this treatment decreases the levels of the de-ubiquitinase, USP9x, thereby resulting in increased turnover of MCL-1 protein and increased β-cell apoptosis.

Figure 1

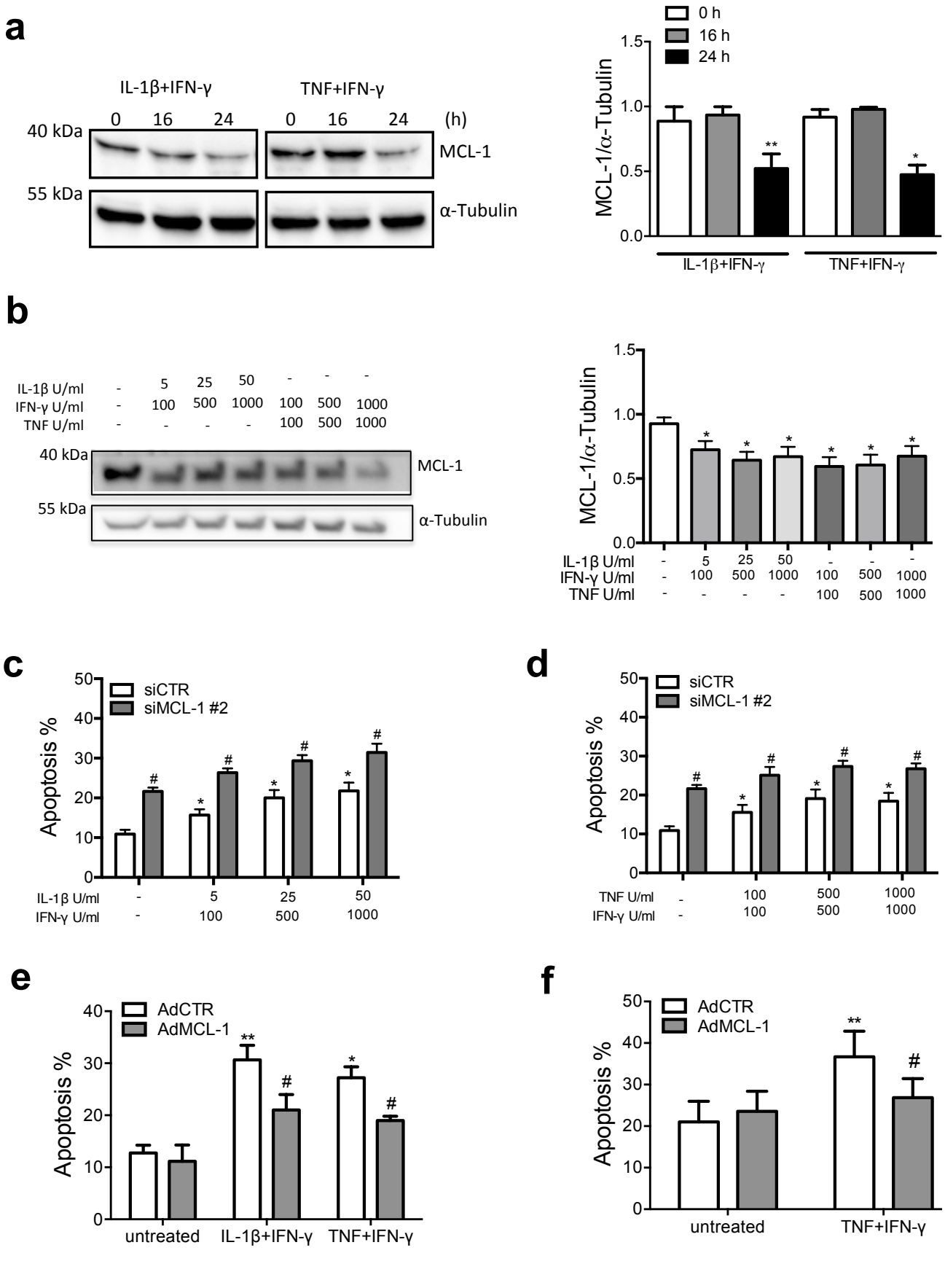
a
IL-1β+IFN-γ
TNF+IFN-γ
0 16 24 0 16 24 (h)
40 kDa
55 kDa
MCL-1
α-Tubulin
0 h
16 h
24 h
MCL-1/α-Tubulin
IL-1β+IFN-γ
TNF+IFN-γ
b
IL-1β U/ml
IFN-γ U/ml
TNF U/ml
c
siCTR
siMCL-1 #2
Apoptosis %
d
e
AdCTR
AdMCL-1
untreated
f

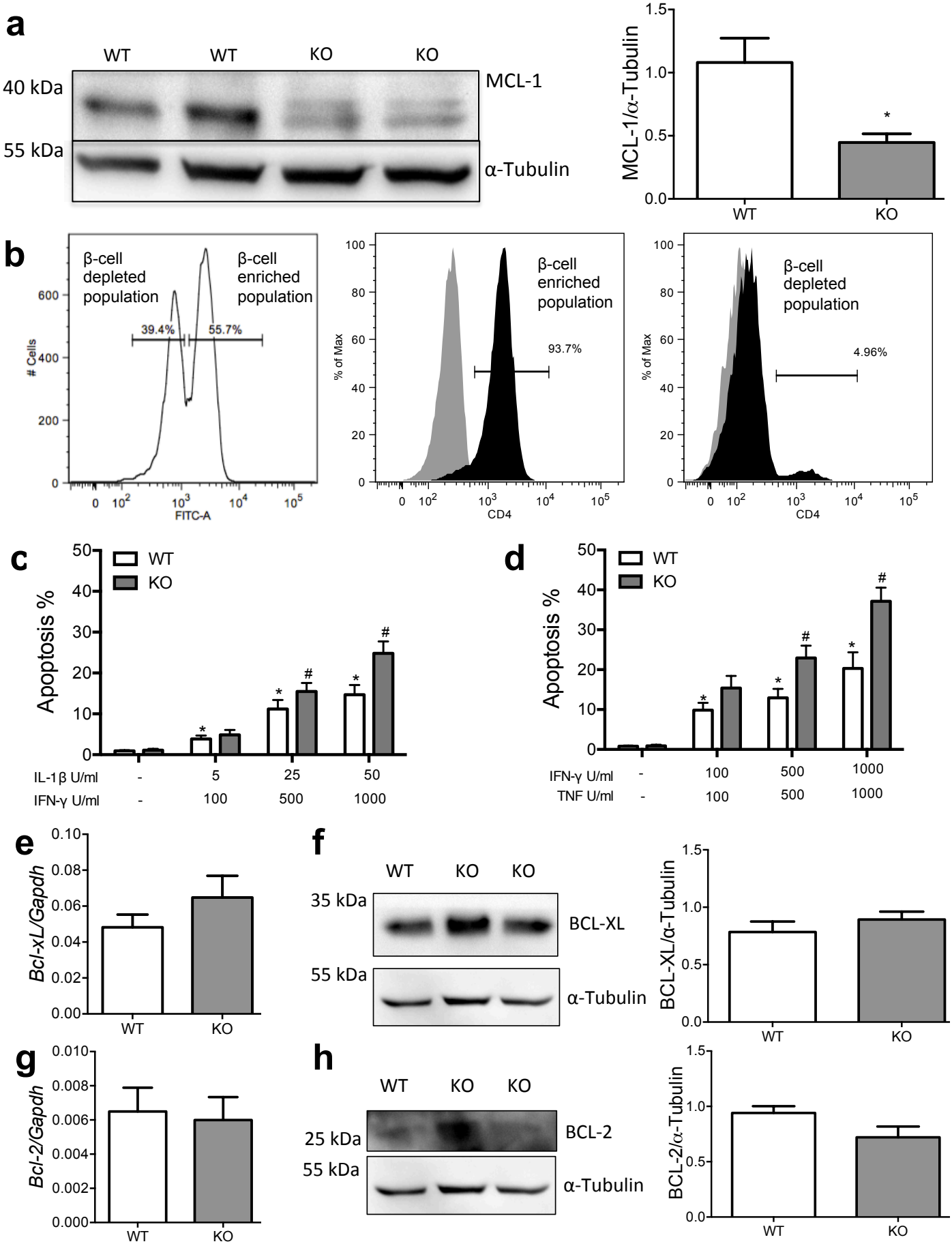
a
WT
WT
KO
KO
40 kDa
55 kDa
MCL-1
α-Tubulin
MCL-1/α-Tubulin
WT
KO
b
β-cell depleted population
β-cell enriched population
39.4%
55.7%
Cells
FITC-A
β-cell enriched population
93.7%
% of Max
CD4
β-cell depleted population
4.96%
% of Max
CD4
c
WT
KO
Apoptosis %
IL-1β U/ml
IFN-γ U/ml
d
WT
KO
Apoptosis %
IFN-γ U/ml
TNF U/ml
e
Bcl-xL/Gapdh
WT
KO
f
WT
KO
KO
35 kDa
55 kDa
BCL-XL
α-Tubulin
BCL-XL/α-Tubulin
g
Bcl-2/Gapdh
WT
KO
h
WT
KO
KO
25 kDa
55 kDa
BCL-2
α-Tubulin
BCL-2/α-Tubulin

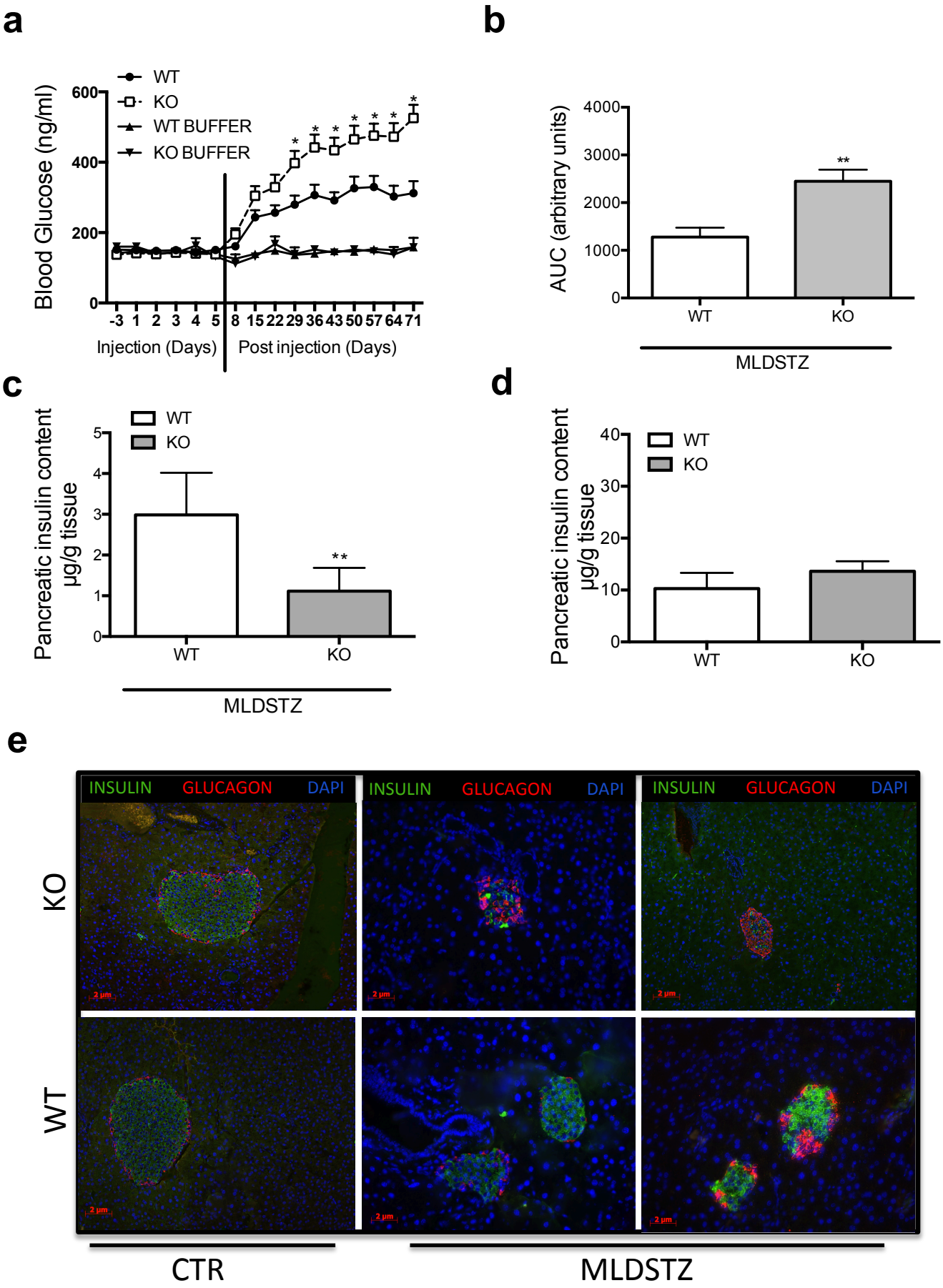
a
WT
KO
WT BUFFER
KO BUFFER
Blood Glucose (ng/ml)
600
400
200
0
-3 1 2 3 4 5 8 15 22 29 36 43 50 57 64 71
Injection (Days)
Post injection (Days)
b
AUC (arbitrary units)
4000
3000
2000
1000
0
**
WT
KO
MLDSTZ
c
Pancreatic insulin content µg/g tissue
WT
KO
5
4
3
2
1
0
**
WT
KO
MLDSTZ
d
Pancreatic insulin content µg/g tissue
WT
KO
40
30
20
10
0
WT
KO
e
INSULIN GLUCAGON DAPI
KO
WT
CTR
MLDSTZ

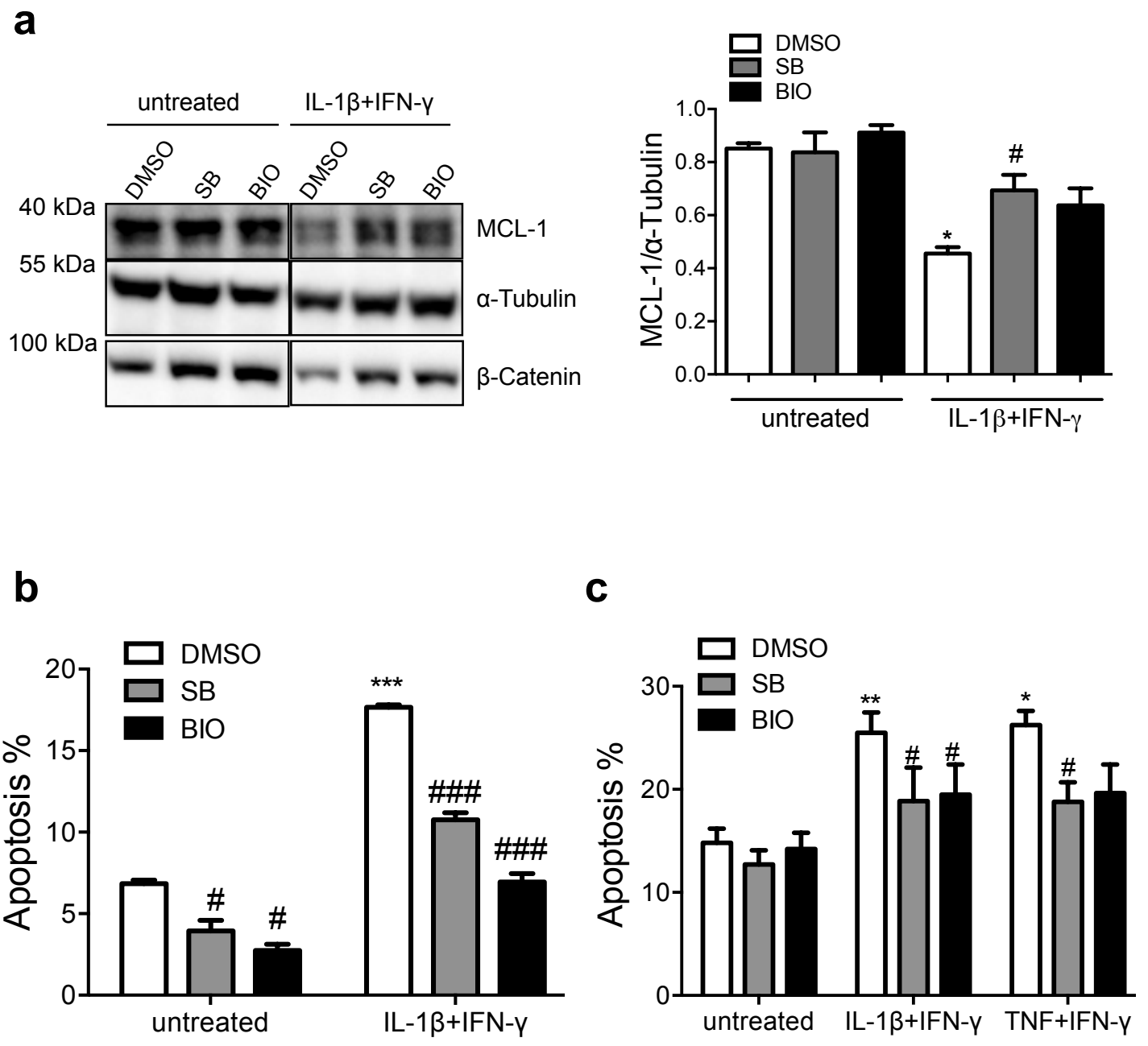
a
untreated
IL-1β+IFN-γ
DMSO
SB
BIO
DMSO
SB
BIO
40 kDa
55 kDa
100 kDa
MCL-1
α-Tubulin
β-Catenin
DMSO
SB
BIO
MCL-1/α-Tubulin
1.0
0.8
0.6
0.4
0.2
0.0
*
#
untreated
IL-1β+IFN-γ
b
DMSO
SB
BIO
Apoptosis %
20
15
10
5
0
***
###
###
#
#
untreated
IL-1β+IFN-γ
c
DMSO
SB
BIO
Apoptosis %
30
20
10
0
**
#
#
*
#
untreated
IL-1β+IFN-γ
TNF+IFN-γ

Figure 5

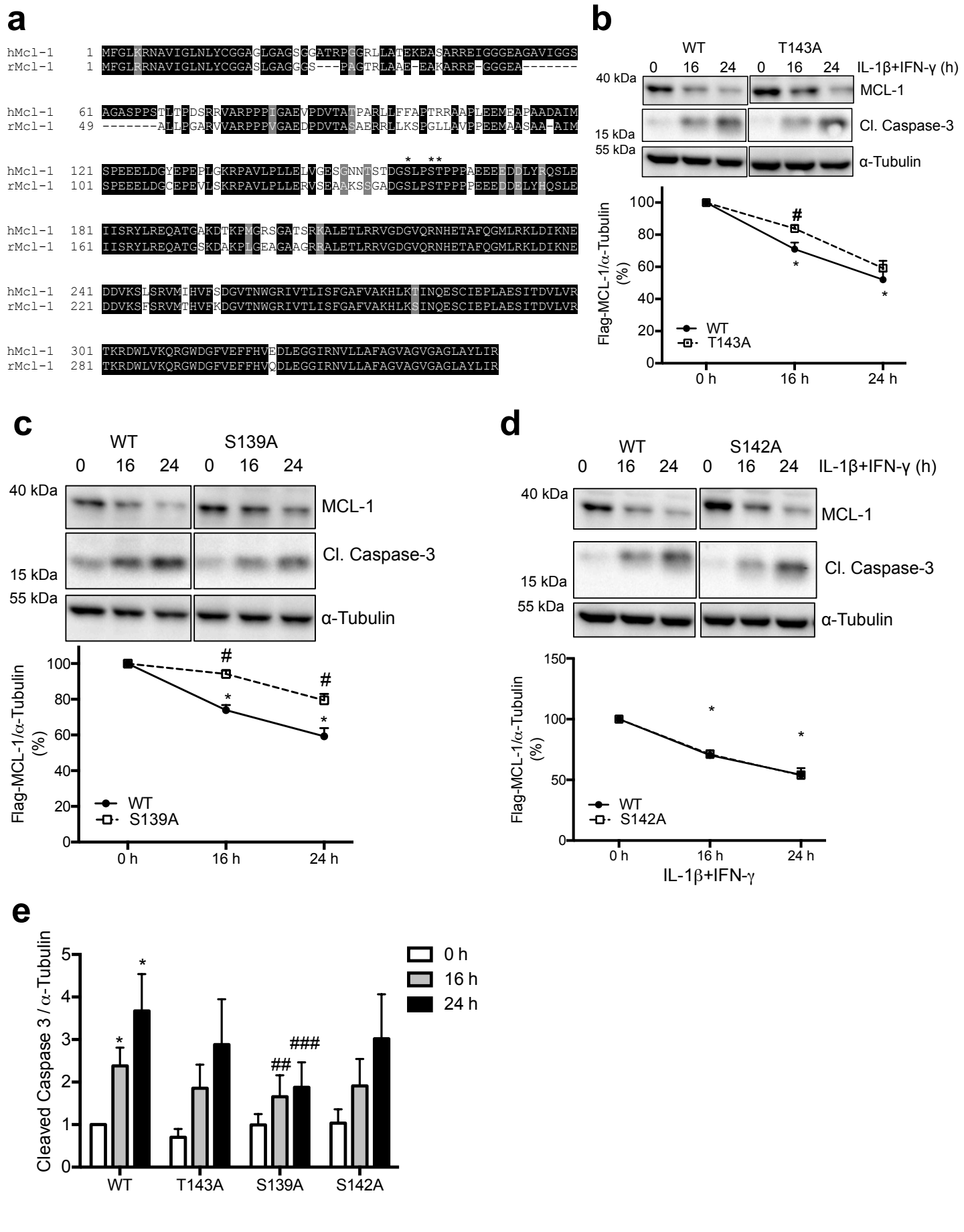
a
hMcl-1 1 MFGLKRNAVIGLNLYCGGAGLGAGSGGATRPGGRLLATEKEASARREIGGGEAGAVIGGS
rMcl-1 1 MFGLRRNAVIGLNLYCGGASLGAGGGS---PAGTRLAAEE-EAKARRE-GGGEA-------
hMcl-1 61 AGASPPSTLTPDSRRVARPPPIGAEVPDVTATPARLLFFAPTRRAAPLEEMEAPAADAIM
rMcl-1 49 -------ALLPGARVVARPPPVGAEDPDVTASAERRLLKSPGLLAVPPEEMAASAA-AIM
hMcl-1 121 SPEEELDCYEPEPLGKRPAVLPLLELVGPSGNNTSTDGSLPSTPPPAEEEEDDLYRQSLE
rMcl-1 101 SPEEELDGCEPEVLSKRPAVLPLLERVSPAAKSSGADGSLPSTPPPPEEEDDELYHQSLE
hMcl-1 181 IISRYLREQATGAKDTKPMGRSGATSRKALETLRRVGDGVQRNHETAFQGMLRKLDIKNE
rMcl-1 161 IISRYLREQATGSKDAKPLGEAGAAGRRALETLRRVGDGVQRNHETAFQGMLRKLDIKNE
hMcl-1 241 DDVKSLSRVMIHVFSDGVTNWGRIVTLISFGAFVAKHLKTINQESCIEPLAESITDVLVR
rMcl-1 221 DDVKSFSRVMTHVFKDGVTNWGRIVTLISFGAFVAKHLKSINQESCIEPLAESITDVLVR
hMcl-1 301 TKRDWLVKQRGWDGFVEFFHVEDLEGGIRNVLLAFAGVAGVGAGLAYLIR
rMcl-1 281 TKRDWLVKQRGWDGFVEFFHVQDLEGGIRNVLLAFAGVAGVGAGLAYLIR
b
WT
T143A
0 16 24 0 16 24 IL-1β+IFN-γ (h)
40 kDa
MCL-1
Cl. Caspase-3
15 kDa
55 kDa
α-Tubulin
Flag-MCL-1/α-Tubulin (%)
WT
T143A
0 h
16 h
24 h
c
WT
S139A
0 16 24 0 16 24
40 kDa
MCL-1
Cl. Caspase-3
15 kDa
55 kDa
α-Tubulin
Flag-MCL-1/α-Tubulin (%)
WT
S139A
0 h
16 h
24 h
d
WT
S142A
0 16 24 0 16 24 IL-1β+IFN-γ (h)
40 kDa
MCL-1
Cl. Caspase-3
15 kDa
55 kDa
α-Tubulin
Flag-MCL-1/α-Tubulin (%)
WT
S142A
0 h
16 h
24 h
IL-1β+IFN-γ
e
Cleaved Caspase 3 / α-Tubulin
0 h
16 h
24 h
WT
T143A
S139A
S142A

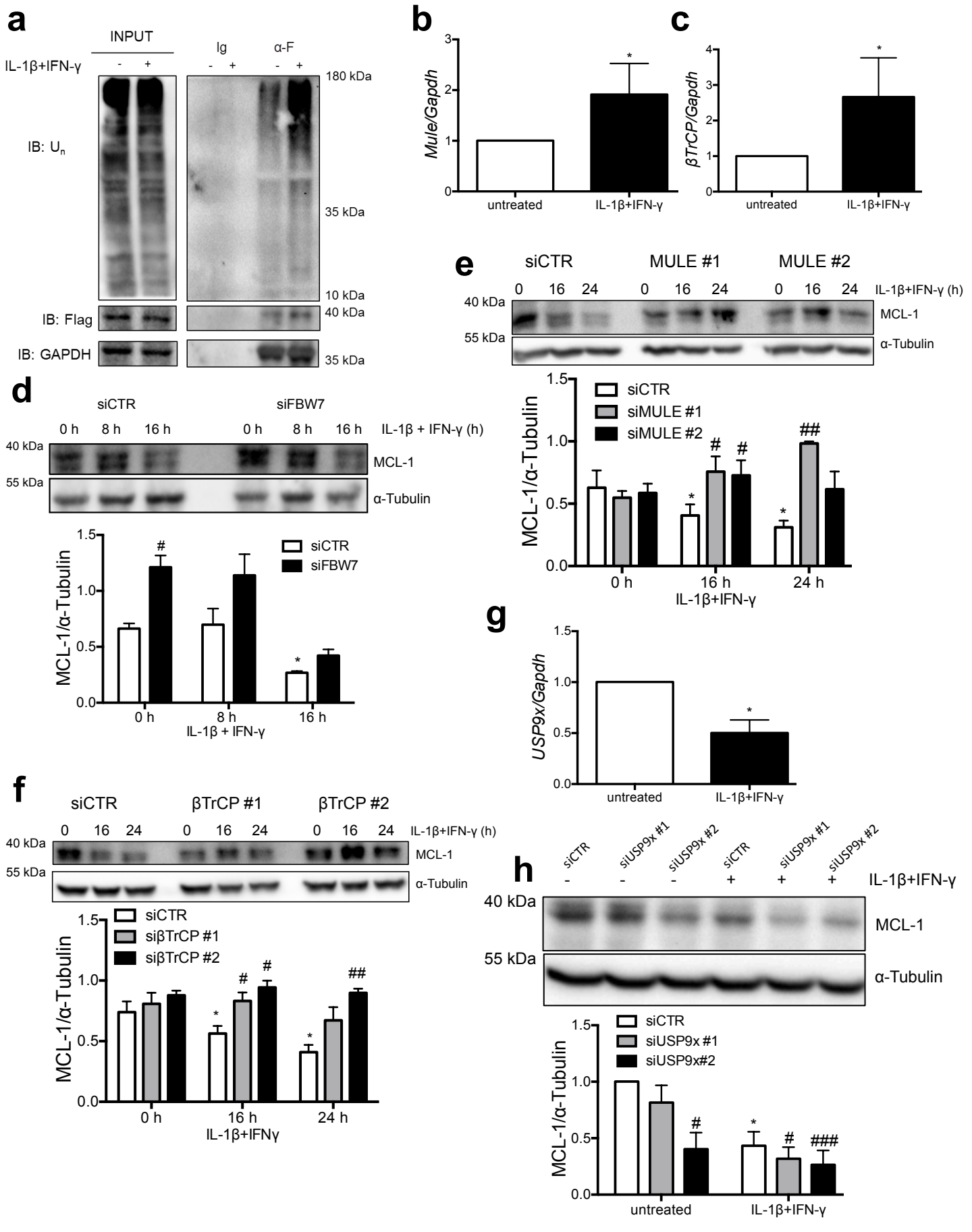
a
INPUT
Ig
α-F
IL-1β+IFN-γ
- + - + - +
180 kDa
IB: Un
35 kDa
10 kDa
IB: Flag
40 kDa
IB: GAPDH
35 kDa
b
Mule/Gapdh
untreated
IL-1β+IFN-γ
c
βTrCP/Gapdh
untreated
IL-1β+IFN-γ
d
siCTR
siFBW7
0 h 8 h 16 h 0 h 8 h 16 h
IL-1β + IFN-γ (h)
40 kDa
MCL-1
55 kDa
α-Tubulin
MCL-1/α-Tubulin
siCTR
siFBW7
0 h
8 h
16 h
IL-1β + IFN-γ
e
siCTR
MULE #1
MULE #2
0 16 24 0 16 24 0 16 24
IL-1β+IFN-γ (h)
40 kDa
MCL-1
55 kDa
α-Tubulin
MCL-1/α-Tubulin
siCTR
siMULE #1
siMULE #2
0 h
16 h
24 h
IL-1β+IFN-γ
f
siCTR
βTrCP #1
βTrCP #2
0 16 24 0 16 24 0 16 24
IL-1β+IFN-γ (h)
40 kDa
MCL-1
55 kDa
α-Tubulin
MCL-1/α-Tubulin
siCTR
siβTrCP #1
siβTrCP #2
0 h
16 h
24 h
IL-1β+IFNγ
g
USP9x/Gapdh
untreated
IL-1β+IFN-γ
h
siCTR
siUSP9x #1
siUSP9x #2
siCTR
siUSP9x #1
siUSP9x #2
- - - + + +
IL-1β+IFN-γ
40 kDa
MCL-1
55 kDa
α-Tubulin
MCL-1/α-Tubulin
siCTR
siUSP9x #1
siUSP9x#2
untreated
IL-1β+IFN-γ

Figure 7

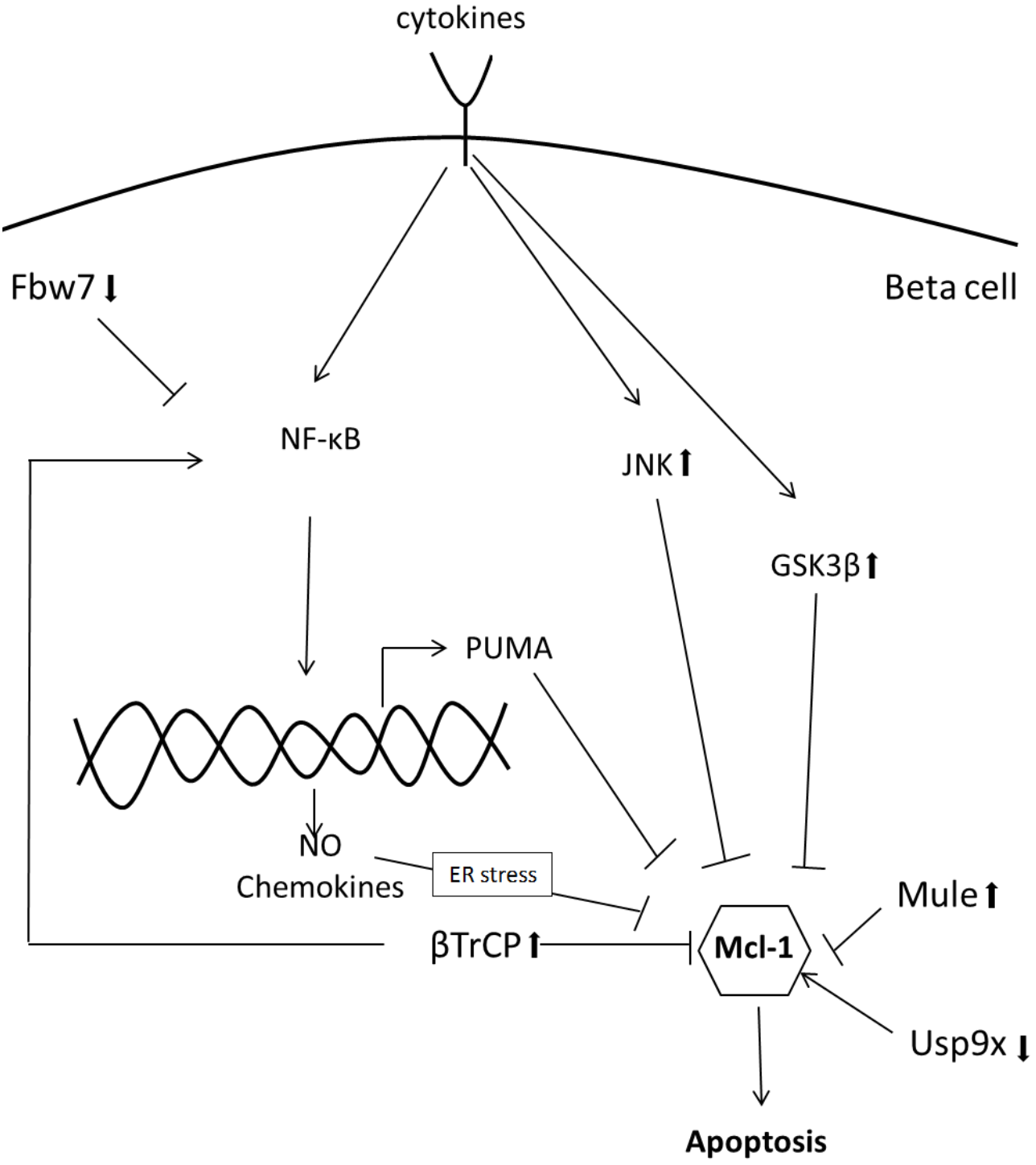
cytokines
Fbw7 ⬇
Beta cell
NF-κB
JNK ⬆
GSK3β ⬆
PUMA
NO
Chemokines
ER stress
Mule ⬆
βTrCP ⬆
Mcl-1
Usp9x ⬇
Apoptosis

Supplemental Figure Legends:

Supplemental Figure 1: Cytokine-induced EndoCβH1 cell apoptosis and ***efficacy of Mcl-1 knockdown and overexpression*****. (a)** EndoCβH1 cells were treated with IL-1β (50 U/mL) +IFN-γ (1000 U/mL) or TNF (1000 U/mL)+IFN-γ (1000 U/mL) for 16h or 24h. Cell viability was assessed by HO/PI staining. *p<0.05 *vs* untreated. **(b-c)** EndoCβH1 cells were transfected with siCTR or *siMcl-1* (#1, #2)**.** *Mcl-1* mRNA expression was analysed by real time RT-PCR (b). *p<0.05 *vs* siCTR. A representative Western blot of MCL-1 and α-tubulin (loading control) of 3 independent experiments (c). (d) EndoCβH1 cells were transfected with siCTR or *siMcl-1* (#1, #2). Cell viability after cytokine treatment was analysed by HO/PI staining. *p<0.05 *vs* siCTR under untreated condition; #p<0.05, ##p<0.01 *siMcl-1 vs* siCTR under respective condition. **(e-f)** EndoCβH1 cells **(e)** and dispersed human islets **(f)** were transduced with a control adenovirus virus (AdCtr) or an adenovirus encoding rat MCL-1 (AdMCL-1) at a multiplicity of infection (MOI) 10. The mRNA expression of rat *Mcl-1* was analysed by real time RT-PCR. Data represent mean ± SEM of 3-6 independent experiments. *p<0,005 Ad *MCL-1 vs* Ad Ctr.

Supplemental Figure 2: ***β-cell specific MCL-1 depletion does not influence glucose metabolism in mice and semi-quantitative analysis of insulin and glucagon staining on sections from islets of MLDSTZ treated βMcl-1KO mice and WT littermates.*** **(a-d)** Intra-peritoneal glucose tolerance tests (ipGTT) were performed in male **(a-b)** and female **(c-d)** *βMcl-1*KO and WT mice at 12 and 24 weeks, as indicated. **(e-f)** Fed glycaemic levels **(e)** and body weight **(f)** of male *βMcl-1*KO mice and WT littermates. **(g)** Islets were isolated from *βMcl-1*KO or WT littermates and glucose stimulated insulin release in response to glucose alone or in combination with forskoline (20 mM) was assessed. *p<0.05 *vs* 2.8 mM WT. #p<0.05 *vs* 16.7 mM WT. **(h)** Total pancreatic insulin content was evaluated in female *βMcl-1*KO and WT littermates at 24 weeks.

Data represent mean ± SEM 4-7 different animals per group. **(i-j)** Representative images of immunofluorescence staining for insulin (green), glucagon (red) and DAPI in islets from WT **(i)** and *βMcl-1*KO **(j)** mice. Scale bars, 2 μm- 40X. **(k)** Percentages of insulin staining area in islets from *βMCL-1*KO mice and WT littermates after MLDSTZ treatment. Grade 1: islets containing 60-80% of insulin-positive cells (normal insulin staining). Grade 2: islets containing 30-59% of insulin-positive cells (insulin-depleted islets). Grade 3: islets containing 10-29% of insulin-positive cells (severely insulin-depleted islets). Grade 4: islets containing 0-9% of insulin-positive cells (near total insulin-depleted islets). More than 60% of islets from WT mice showed grade 2 and more than 20% showed grade 3. Conversely, in islets from *βMcl-1*KO mice around 60% were grade 3 and almost 40% grade 4, indicating decreased insulin staining as compared to WT islets. (l) Percentages of glucagon staining area in islets from *βMcl-1*KO mice and WT littermates after MLDSTZ treatment. Grade 1: islets containing 0-5% of glucagon-positive cells (glucagon-depleted islets). Grade 2: islets containing 6-15% of glucagon-positive cells (normal glucagon staining). Grade 3: islets containing 16-70% of glucagon-positive cells (increased glucagon levels). Grade 4: islets containing >71% of glucagon-positive cells (increased glucagon levels). Around 40% of the islets from WT mice showed grade 2, while 40% showed grade 3. In contrast, around 70% of the islets from the *βMcl-1*KO showed grade 4. These results are in line with, and probably reflect, the increased depletion of insulin positive cells in the islets from the KO mice.

Supplemental Figure 3: ***Mcl-1 mRNA expression is induced by inflammatory cytokines in EndoCβH1 cells and ectopically expressed MCL-1 protein has the same degradation kinetics as the endogenous MCL-1 protein in cells exposed to cytokines.*** (a) EndoCβH1 cells were treated with IL-1β+IFN-γ for up to 24h, as indicated, and the expression of *MCL-1* mRNA was

analysed by real time RT-PCR. *p<0.05 *vs* untreated (0h). **(b)** INS-1E cells were transfected or not with an expression vector encoding for rat MCL-1 (pExpress-MCL-1) and exposed to IL-1β+IFN-γ for different time points, as indicated. Expression of endogenous MCL-1 (from non-transfected INS-1E cells) and ectopically expressed (obtained by transient transfection with pExpress-MCL-1) was analysed by Western blotting and data are represented as densitometric assessment **(b)** INS-1E cells were transfected with expression constructs encoding WT Flag-MCL-1 from rat (WT) or the indicated Flag-MCL-1 mutants and Flag-MCL-1 expression was analysed under basal condition by Western blotting and data are represented as densitometric assessment. Data represent mean ± SEM of 3-5 independent experiments.

Supplemental Figure 4: ***Efficacy of the knockdown of Mule, βTrCP and USP9x.*** **(a-f)** INS-1E cells were transfected with siCTR (control siRNA), *siMule* (#1, #2) **(a-b)**, *siβTrCP* (#1, #2) **(c-d)** or *siUSP9x* (#1, #2) **(e-f)** and treated with IL-1β+IFN-γ for 16h, as indicated. *Mule* **(a)**, *βTrCP* **(b)** and *USP9x* **(c)** mRNA expression levels were analysed by real time RT-PCR. A representative Western blot of MULE **(b)**, βTrCP **(d)** and USP9x **(f)** and α-tubulin (loading control) expressions under untreated condition of at least 3 independent experiments is shown. *p<0.05, ***p<0.001 siCTR cytokines *vs* siCTR under untreated conditions, #p<0.05, ##p<0.01, ###p<0.001 siUSP9x, *siMule* or *siβTrCP vs* siCTR, under the respective conditions. Data represent mean ± SEM of 3-4 independent experiments.

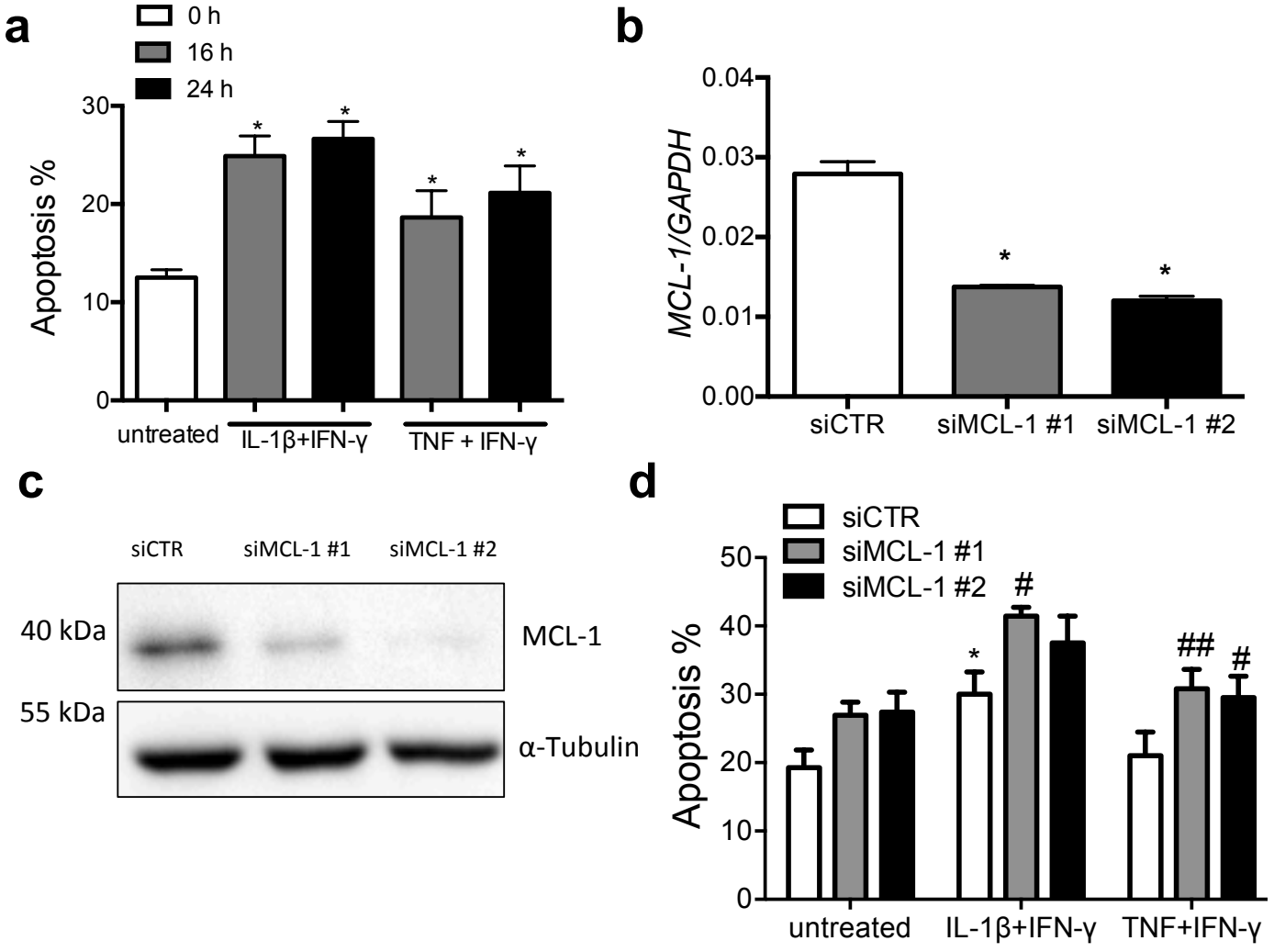
a
0 h
16 h
24 h
Apoptosis %
untreated
IL-1β+IFN-γ
TNF + IFN-γ
b
MCL-1/GAPDH
siCTR
siMCL-1 #1
siMCL-1 #2
c
siCTR
siMCL-1 #1
siMCL-1 #2
40 kDa
MCL-1
55 kDa
α-Tubulin
d
siCTR
siMCL-1 #1
siMCL-1 #2
Apoptosis %
untreated
IL-1β+IFN-γ
TNF+IFN-γ
e
Mcl-1/Gapdh
AdCTR
AdMCL-1
f
Mcl-1/Gapdh
AdCTR
AdMCL-1

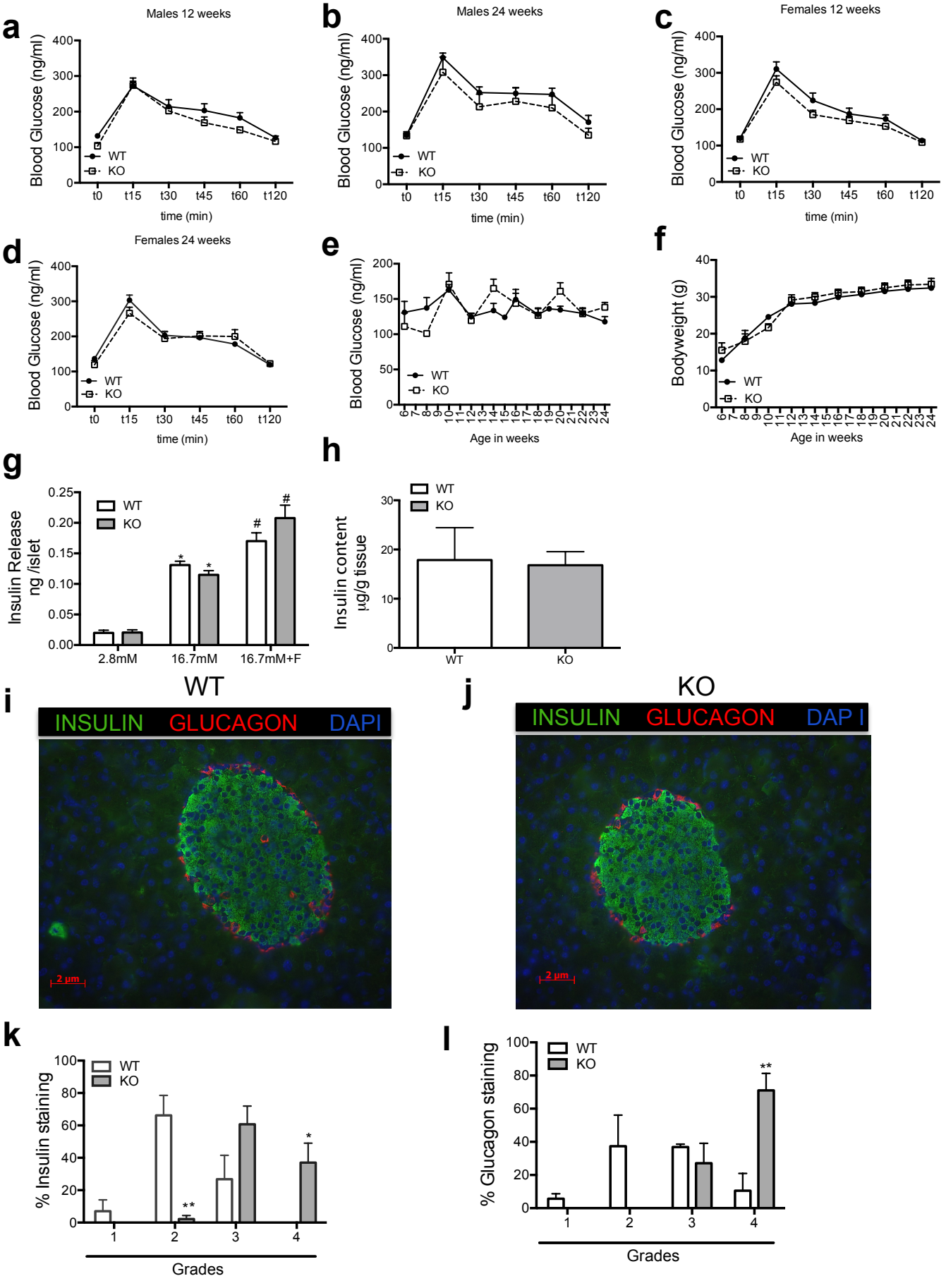
a
Males 12 weeks
Blood Glucose (ng/ml)
WT
KO
t0 t15 t30 t45 t60 t120
time (min)
b
Males 24 weeks
c
Females 12 weeks
d
Females 24 weeks
e
Age in weeks
f
Bodyweight (g)
g
Insulin Release ng /islet
2.8mM
16.7mM
16.7mM+F
h
Insulin content µg/g tissue
i
WT
INSULIN GLUCAGON DAPI
2 µm
j
KO
INSULIN GLUCAGON DAP I
k
% Insulin staining
Grades
l
% Glucagon staining

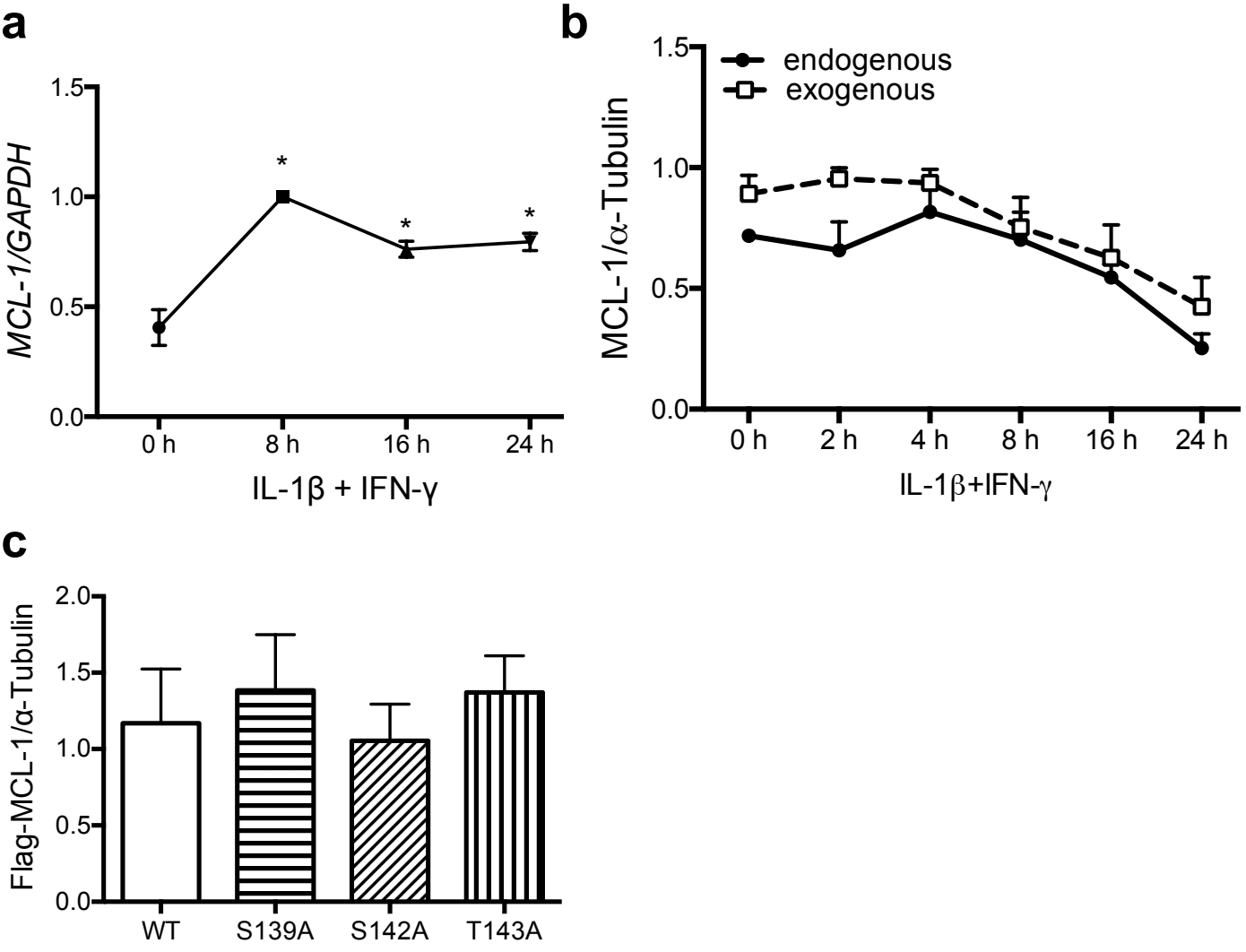
a
MCL-1/GAPDH
1.5
1.0
0.5
0.0
*
*
*
0 h
8 h
16 h
24 h
IL-1β + IFN-γ
b
MCL-1/α-Tubulin
1.5
1.0
0.5
0.0
endogenous
exogenous
0 h
2 h
4 h
8 h
16 h
24 h
IL-1β+IFN-γ
c
Flag-MCL-1/α-Tubulin
2.0
1.5
1.0
0.5
0.0
WT
S139A
S142A
T143A

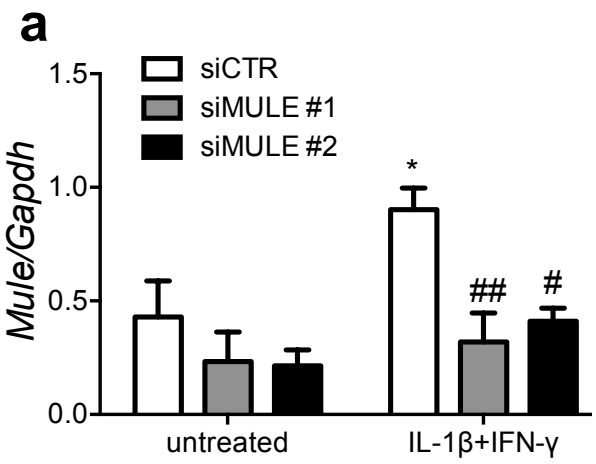
a
siCTR
siMULE #1
siMULE #2
Mule/Gapdh
1.5
1.0
0.5
0.0
*
##
#
untreated
IL-1β+IFN-γ

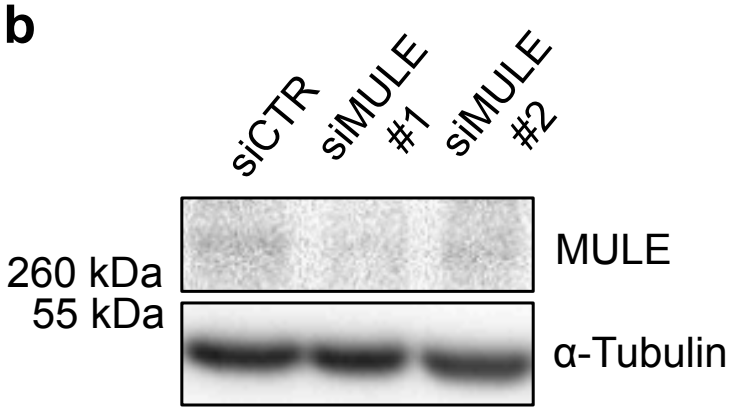
b
siCTR
siMULE #1
siMULE #2
260 kDa
55 kDa
MULE
α-Tubulin

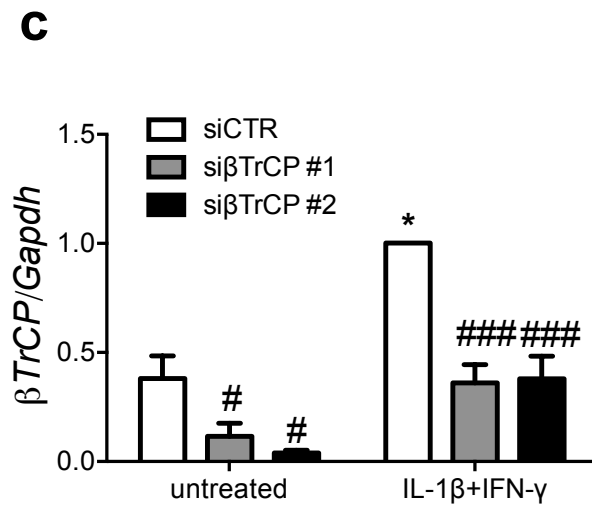
c
siCTR
siβTrCP #1
siβTrCP #2
βTrCP/Gapdh
1.5
1.0
0.5
0.0
*
#
#
###
###
untreated
IL-1β+IFN-γ

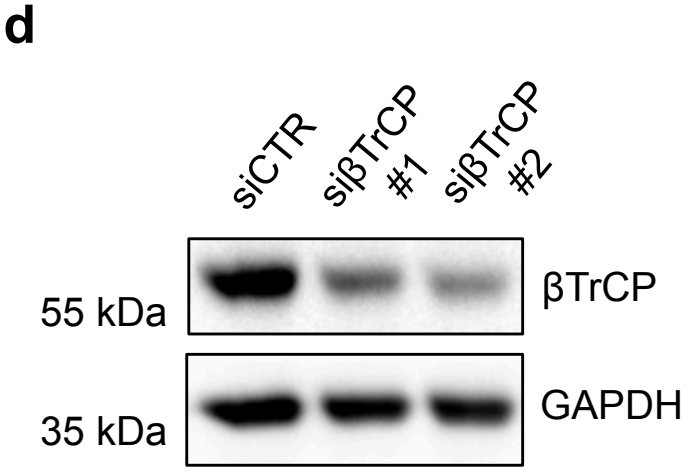
d
siCTR
siβTrCP #1
siβTrCP #2
55 kDa
35 kDa
βTrCP
GAPDH

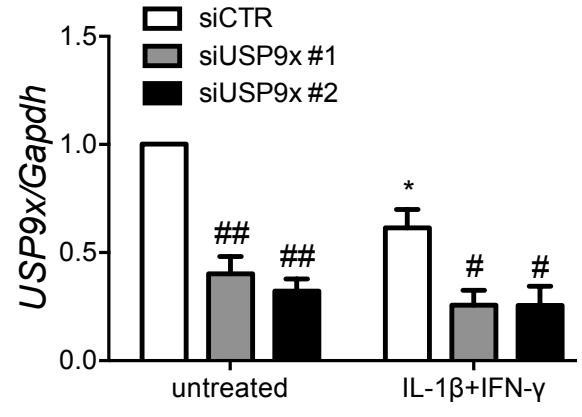
e
siCTR
siUSP9x #1
siUSP9x #2
USP9x/Gapdh
1.5
1.0
0.5
0.0
##
##
*
#
#
untreated
IL-1β+IFN-γ

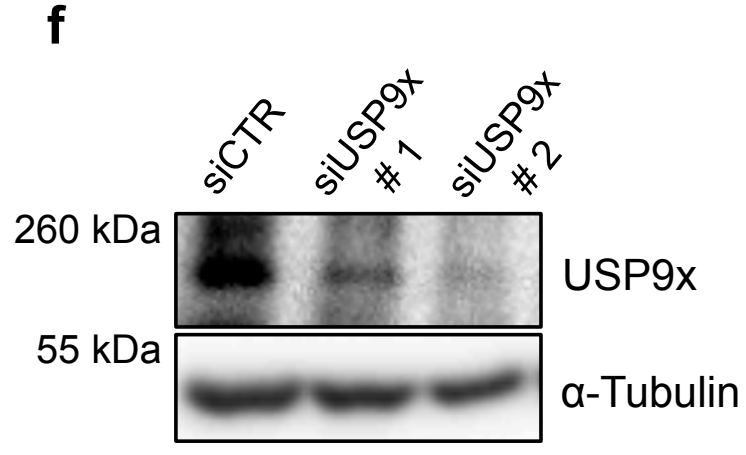
f
siCTR
siUSP9x #1
siUSP9x #2
260 kDa
55 kDa
USP9x
α-Tubulin

Supplemental Table 1

List of cytokines and concentrations used in the experiments

Cytokine	Cell type	Concentration	Company
Recombinant human IL-1β	INS-1E cells EndoCβH1/ mouse islets	10 U/mL 5-50 U/mL	R&D Systems, Abingdon, UK
Recombinant rat IFN-γ	INS-1E cells	36 ng/mL	R&D Systems, Abingdon, UK
Recombinant mouse IFN-γ	Mouse islets	100-1000 U/mL	PeproTech, RockyHill, USA
Recombinant human IFN-γ	EndoCβH1 and human islets	100-1000 U/mL	PeproTech, RockyHill, USA
Recombinant murine TNF	INS-1E cells/ EndoCβH1/ mouse and human islets	100-1000 U/mL	Innogenetics, Ghent, Belgium

Supplemental Table 2

List of antibodies used in the Western blot or immunofluorescence analysis

Antibody	**Company**	**Reference**
MCL-1	Biovision (Abingdon, UK)	3035-100
α-tubulin	Sigma (Diegem, Belgium)	T9026
GAPDH	Trevigen (Gaithersburg, USA)	2275PC100
Insulin	Sigma (Diegem, Belgium)	I2018
Glucagon	Sigma (Diegem, Belgium)	G2654
β-catenin	Santa Cruz (Heidelberg, Germany)	Sc-133239
FLAG	Sigma (Diegem, Belgium)	F3564
Cl. caspase 3	Cell Signaling (Leiden, Netherlands)	9661
BCL-2	Cell Signaling (Leiden, Netherlands)	2870
BCL-XL	Cell Signaling (Leiden, Netherlands)	2764
MULE	Cell Signaling (Leiden, Netherlands)	5695
β-TrCP	Cell Signaling (Leiden, Netherlands)	11984
USP9x	Cell Signaling (Leiden, Netherlands)	5571

Supplemental Table 3

List of the sequences of the used siRNAs and primers

siRNAs	**Sequence sense (5'-3')**	**Sequence antisense (5'-3')**
Human Mcl-1 #1	Sequence is not provided (Ambion, Alst, Belgium, Cat # 1299001, HSS181042)	
Human Mcl-1 #2	Sequence is not provided (Ambion, Alst, Belgium, Cat # 1299001, HSS181043)	
Rat FBW7 #1	CGUUAACAAGUGGAAUGGAACUCAA	UUGAGUUCCAUUCCACUUGUUAACG
Rat FBW7 #2	UCGUUACAGUUUGACGGCAUCCAUG	CAUGGAUGCCGUCAAACUGUAACGA
Rat USP9x #1	GAGAUGGAGCAAGAGUUCUUAUGAA	UUCAUAAGAACUCUUGCUCCAUCUC
Rat USP9x #2	GGAGAAUCCUCAGUUCUCAUCUACU	AGUAGAUGAGAACUGAGGAUUCUCC
Rat Mule #1	UAAAGUGGCUGGGAAAUACCUUGGC	GCCAAGGUAUUUCCCAGCCACUUUA
Rat Mule #2	CAAAGUUGAAGAAAUCAGUACGCUG	CAGCGUACUGAUUUCUUCAACUUUG
Rat βTrCP #1	CCAUGAGGAAUUGGUACGCUGUAUU	AAUACAGCGUACCAAUUCCUCAUGG
Rat βTrCP #2	GCAGCGGAAACUCUCAGCAAGCUAU	AUAGCUUGCUGAGAGUUUCCGCUGC
Real time PCR primers	**Sequence sense (5'-3')**	**Sequence antisense (5'-3')**
Rat USP9x	GAAGGGGTGCCTACCTCAA	GCCTTCTACACCTGGCTGAC
Rat βTrCP	TCAGGCTGTGGGACATAGAG	GGTCCAGAGCAGCCATAAGA
Rat FBW7	GCTGGAGTGGACCAGAGAAG	GGGGAGCAAGGAGATGAAGT
Rat Mcl-1	CCTCCAGCCACCAACTACAT	CCACTTTCTTTCTGCCGTGTTA
Human Mcl-1	CCATCATGTCGCCCGAAGAGG	TACCAGATTCCCCGACCAACTCCA
Rat GAPDH	GCCTGGAGAAACCTGCCAAGTATGA	AACCTGGTCCTCAGTGTAGCCC
Human GAPDH	CAGCCTCAAGATCATCAGCA	TGTGGTCATGAGTCCTTCCA
Mouse Bcl-2	TCGCTACCGTCGTGACTTCG	TTCCTCCACCACCGTGGCAA
Mouse Bcl-xL	TGGCAGCAGTGAAGCAAGCG	AGTGCCCCGCCAAAGGAGAA
Site-directed mutagenesis primers	**Sequence sense (5'-3')**	**Sequence antisense (5'-3')**
S139	AGCTGACGGCGCGCTGCCCTCCA	CCGGAGCTCTTAGCCGCCTCG
S142	CTCGCTGCCCGCCACGCCGCCGC	CCGTCAGCTCCGGAGCTCTTAGCCGC
T143	GCTGCCCTCCGCGCCGCCGCCGC	GAGCCGTCAGCTCCGGAGCTCTTAGCCGC